NASA Technical Paper 3448

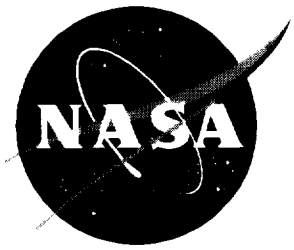

Baseline Tests of an Autonomous Telerobotic System for Assembly of Space Truss Structures

Marvin D. Rhodes and Ralph W. Will
Langley Research Center • Hampton, Virginia

Coung Quach
Lockheed Engineering & Sciences Company • Hampton, Virginia

National Aeronautics and Space Administration
Langley Research Center • Hampton, Virginia 23681-0001

July 1994

Abstract

Several proposed space missions include precision reflectors that are larger in diameter than any current or proposed launch vehicle. Most of these reflectors will require a truss structure to accurately position the reflector panels and these reflectors will likely require assembly in orbit. A research program has been conducted at the NASA Langley Research Center to develop the technology required for the robotic assembly of truss structures. The focus of this research has been on hardware concepts, computer software control systems, and operator interfaces necessary to perform supervised autonomous assembly. A special facility was developed and four assembly and disassembly tests of a 102-strut tetrahedral truss have been conducted. The test procedures were developed around traditional "pick-and-place" robotic techniques that rely on positioning repeatability for successful operation. The data from two of the four tests were evaluated and are presented in this report. All operations in the tests were controlled by predefined sequences stored in a command file, and the operator intervened only when the system paused because of the failure of an actuator command. The tests were successful in identifying potential pitfalls in a telerobotic system, many of which would not have been readily anticipated or incurred through simulation studies. Addressing the total integrated task, instead of bench testing the component parts, forced all aspects of the task to be evaluated. Although the test results indicate that additional developments should be pursued, no problems were encountered that would preclude automated assembly in space as a viable construction method.

Introduction

Several proposed space missions include precision reflectors that are larger in diameter than any current or proposed launch vehicle. An example of one proposed reflector that is anticipated to be a key instrument in deep-space astrophysics research is the submillimeter astronomical telescope described in reference 1 and illustrated in figure 1. The telescope reflector will require a precision truss structure to position the reflector panels for the required optical resolution. The truss structure may incorporate hundreds of members, and because of its size, the truss is likely to require assembly in orbit. Several methods of assembly have been proposed. These methods include member-by-member installation performed by pressure-suited astronauts during extravehicular activity (EVA), assembly of deployable cells or subunits performed by astronauts during EVA, and member-by-member machine assembly performed by special robotic manipulators. The robotic method offers potential advantages over the other proposed methods for assembly in space because robotic systems can operate continuously for long periods and do not involve any risk to humans. If a robotic system were fully automated, the assembly operations could be remotely monitored by an astronaut within a space station or by a terrestrially based operator. Remotely monitored systems are frequently developed around the principle of supervised autonomy and only require assistance or intervention when a problem is encountered. Supervised autonomous assembly is promising for the construction of large space structures; however, little or no development of the methods required for the construction tasks have been performed.

A research program has been conducted at the Langley Research Center (LaRC) to develop the operational requirements for supervised autonomous telerobotic construction of truss structures. This program focused on assembling a tetrahedral truss using struts that are nominally 2 m in length. The program employed traditional industrial robots and many standard robotic techniques. The objectives of the program were: (1) to obtain some practical experience in the development of an automated system for truss assembly tasks, (2) to develop a software system that is capable of reliably performing required tasks and handling realistic error conditions, and (3) to provide an interface that efficiently accommodates the volume of internal information necessary for the operator to maintain supervision of

system operations and truss assembly status. The tests described herein were performed to establish a database of traditional robotic techniques and to provide practical insight into the technologies that need to be enhanced for robotic systems to be capable of performing complex assembly tasks with the reliability necessary for space operations.

Four assembly tests of the 102-strut truss were conducted, and each was followed by a disassembly test. Tests 1 and 2 were preliminary, and several minor hardware and software modifications resulted from them. The results of tests 3 and 4 are reported and discussed in this paper. The time required to perform the various segments of the truss assembly was measured, and the automated operational procedures are reviewed and discussed. The types of errors encountered, the ability of the operator to resolve errors, and the time for error resolution are also discussed.

Symbols and Abbreviations

DOF	degree of freedom
EVA	extravehicular activity
I/O	input/output
rms	root mean square
U, V, W	robot base coordinate system
X, Y, Θ	motion-base coordinate system
x', y', z'	robot tool frame coordinate system (end-effector axis system)
σ	standard deviation

Truss, Test Facility, and Assembly Operations

The test facility developed to perform the automated assembly of truss structures is shown in figure 2. Figure 2(a) shows the actual truss support structure and test system, and figure 2(b) identifies some of the components. The facility is a research tool to develop the basic techniques for joining struts and evaluating end-effector mechanisms, computer software control systems, operational procedures, and operator interface requirements. A large tetrahedral truss structure that is assembled on a one-degree-of-freedom (1 DOF) rotational motion base by an anthropomorphic 6 DOF robot mounted on a 2 DOF Cartesian motion base comprise the test facility hardware. An end effector mounted to the wrist of the robot is used to both acquire struts from pallets stored in a canister and install the struts in the truss structure. The Cartesian and rotational motion bases expand the working envelope of the robot to provide a 9 DOF manipulator system. Many of the components in the test facility, including the robot, were obtained commercially to expedite development and minimize cost.

Three coordinate systems are necessary to define the position and orientation of the truss members and to describe operations of the test facility. The coordinate systems, shown in figure 2(b), are the motion-base coordinate system X, Y, Θ; the robot base coordinate system U, V, W; and the robot tool frame (end-effector axis system) x', y', z'. The motion-base coordinate system (X, Y, Θ) defines the location of the robot base system origin with respect to the rotational axis of the truss. The origin of the robot base system is at the intersection of its waist and shoulder axes. The robot tool frame coordinates (x', y', z') have their origin at the centerline of a strut mounted in the end effector at the install location, as indicated in u figure 2(b). The x'-axis is aligned along the robot forearm and yaw, pitch, and roll of the end effector are a 3-2-1 Euler rotation sequence. The Euler sequence begins with the tool frame aligned with the robot base system.

Truss

The truss is shown mounted on the rotating motion base in figure 2(a). The truss is composed of 102 struts, all nominally 2 m in length, and 31 nodes that connect the struts together. Each node in the truss may connect up to nine struts; six struts lie in a face plane (either top or bottom face) and three core struts connect the face planes together. The struts in the top face form a hexagonal boundary that has 4-m-long sides and 8 m between opposite vertices. The distance between the top and bottom faces is 1.63 m.

Photographs of a typical truss joint and node are shown in figure 3. The joint is composed of two parts. One part is the connector, which contains the mechanical locking components (connector plunger, locking nut, and associated internal mechanisms). The connector is bonded into the end of a 2.64-cm-diameter graphite-epoxy strut tube. The other part is a receptacle that is mechanically attached to a specially machined truss node. For strut assembly, the connector plunger is pushed into the receptacle and the joint is secured by turning the locking nut, drawing the connector plunger toward the connector face, and seating it in a pocket machined within the receptacle. The connector applies a preload across

the receptacle and connector interface so that the assembled structure will have a predictable linear static and dynamic response.

Both the joint and the node are fabricated from aluminum. The joint has a lower axial stiffness (EA) and a larger mass per unit length than the graphite-epoxy tube. Structural considerations require that the length of the joints be as short as possible to minimize the truss mass and the effect of the axial stiffness reduction. The joint length (connector and receptacle) is 9.8 cm and the total joint mass (including the mass of the receptacle) is 134 g. The nodes were also made as small as possible to minimize the mass. The length of the joint and the size of the node were minimized for structural considerations; however, the smaller size reduces joint accessibility and has a significant effect on the design and operation of the end effector, which will be discussed later.

An alignment and grasp adapter is shown to the right of the joint connector in figure 3. The adapter, fabricated from aluminum, is an interface fitting that axially and circumferentially aligns the strut in the end effector. The hexagonal shape assists the circumferential alignment, and the vee groove fits into a protrusion on the end effector to assist the axial alignment. The joint receptacle has a similar vee groove machined into the circumference about 3.2 cm from the end. The entry face of the receptacle, the receptacle vee groove, and the adapter vee groove provide passive positioning alignment for the end effector during strut acquisition and installation.

The components of the truss were manually assembled and the location of the 19 nodes in the top face were measured with respect to a best-fit plane using photogrammetry techniques. The test results indicated that the 19 nodes had a root-mean-square (rms) deviation of 0.014 cm from a best-fit plane, and the largest planar positioning error was 0.025 cm. The rms positioning repeatability for two assembly tests with all struts assembled at the same locations was about 0.005 cm. Additional information about these tests and the truss design can be found in reference 2. The sizes of the test model and struts are representative of those required to support reflector panels of an astronomical telescope; however, the struts are of equal nominal length and the nodes in the top and bottom faces approximate a planar surface instead of a parabolic contour. The planar test model was selected for this assembly study because it was relatively simple to design and fabricate. The repeatability of the strut positions and orientations also minimized the effort required to install the struts with traditional pick and place robotic methods.

Test Facility

Robot and Motion Bases

The robot shown in figure 2 is an electrically driven 6-DOF anthropomorphic industrial manipulator that was selected for its reach envelope, payload capacity, and positioning repeatability. The robot has three revolute joints located at the waist, shoulder, and elbow and also has a 3 DOF spherical wrist. The arm has a maximum reach of about 147 cm, which is achieved with a 103-cm-long forearm and a 44-cm-long upper arm. The robot is mounted on an electrically driven X-Y Cartesian motion base, which provides a translational range of approximately 6.1 m in both the X- and Y-directions. The motion-base locations are measured by using linear encoders, and the positioning repeatability of both bases has been determined experimentally to be ± 0.05 mm. The rotating motion base is powered by an electric motor through a reduction system and has ± 3 revolutions from the reference position. The positioning repeatability of the turntable was determined experimentally to be within ± 0.25 mm at a radial distance of 6.1 m. The Cartesian and the rotational motion bases were designed to minimize the effect of static deformations on positioning repeatability. The static deformations result from moving the base of the robot, moving the strut from the supply canister on the Cartesian motion base to the rotational motion base, and changing the robot arm position and end effector orientation. Details of the motion-base design can be found in references 3 and 4.

To measure the loads on the end effector, a commercial six-axis force-torque load cell was mounted between the robot tool plate and the end effector. The forces and moments were used for the operator display and to reposition the robot arm to relieve forces on the end effector.

End Effector

The end effector used to install and remove members from the truss is a special purpose tool that mounts to the robot tool plate and was designed to be fully compatible with the strut joint connector. A photograph of the end effector is shown in figure 4 and the installation of a strut between two nodes is illustrated by the artist sketch in figure 5. The strut is held by the end effector with the strut holders, which close around the alignment and grasp adapter. The strut holder is locked by a lead screw and driven by a motor, and the jaws are opened by springs. The end effector can be moved toward a strut, and when the jaws contact the adapter fitting, they are forced closed by overcoming the spring opening load. This

feature permits the jaws to be locked or unlocked in the closed position so that strut pickup by the end effector does not have to be coordinated with robot positioning. When the jaws are locked, the strut is clamped in the end effector and no appreciable axial or circumferential free-play occurs.

For strut installation, the end effector is moved toward the joint receptacle and the receptacle fingers are closed around the vee groove. Both the contour of the finger and the vee groove provide passive guidance for realigning the end effector by using the force-torque load cell. Axial position errors of approximately ± 0.7 cm can be accommodated by the vee groove, and displacement and orientation errors of approximately ± 2.5 cm in the $x'z'$-plane at the receptacle can be accommodated by the receptacle fingers. After the fingers are closed and the positioning errors are corrected, the platforms shown in figure 4 advance along the x'-axis and push the connector into the joint receptacle. The platforms are equipped with analog potentiometers to detect position. All other end-effector mechanisms are equipped with simple sensors, such as microswitches, to monitor the response of each command. Although they are not suitable for space operation, pneumatic cylinders are used as end-effector actuators to minimize the mass. All other basic operational concepts of the end effector are suitable for space operations. The mass of the end effector with a strut is about 6 kg.

Strut Storage

The struts are stored in nine pallets stacked in a canister directly behind the robot arm as shown in figure 2. Several pallets partially filled with struts are shown in figure 6 along with an enlarged view of the struts positioned and secured in a pallet. Each pallet holds 13 struts with approximately 1.9 cm between the individual graphite-epoxy tubes in a pallet. When a pallet is empty, it is moved to the storage canister on the left side of the robot (fig. 2). To align and hold the struts in the pallets, a second alignment and positioning adapter is bonded to the strut tube. This adapter interfaces with vertical positioning pins on each side of the strut and the positioning pins are fitted with spring-loaded pin plungers. The pin plungers contact the adapter slightly above the tube centerline; therefore, a vertical force is required to extract each strut from its storage location. This feature is incorporated to lock the pallets together in both the supply and the storage locations. The tops of the positioning pins are chamfered to passively guide the pin into the alignment adapter when the struts are inserted into the pallets during disassembly. The struts are oriented circumferentially with a flat side of the hexagonal adapter resting against the pallet frame. The pallets are stacked so that the stored struts are prevented from rotating or being ejected from the pallet because of vibration. The pallets are aluminum frames with cylindrical handles on each end. The handles have positioning and alignment adapters to permit the pallets to be moved by the end effector in the same manner as the struts.

All struts are installed in the pallets and their location in the pallet is coordinated with the assembly sequence. Nodes are preattached to selected core struts. The receptacles installed on the nodes require a considerable amount of space, and two struts with nodes preattached cannot be placed in adjacent pallet slots. Therefore, a special stacking arrangement was devised and coordinated with the assembly sequence. The stacking arrangement is illustrated in figure 7. In pallet 1, the arrangement has four core struts with preattached nodes located at the top of the stack. These core struts are located in the two outermost slots and at intermediate slots equally spaced between the side positions. Three struts without nodes are located between each of the struts with preattached nodes. Pallet 2 has the same sequence as pallet 1; however, the core struts with preattached nodes are located on the opposite end of the pallet. Pallet 3 has three core struts with preattached nodes, and these nodes are located to fit between those of pallet 1, which is above it. Pallet 4 is similar to pallet 3 except that the nodes are on the same end as those of pallet 2 and nest between them. The struts in pallet 5 are identically arranged to those in pallet 1, and the four-pallet pattern is repeated. The complete 102-strut truss is packaged in 9 pallets; however, 15 positions in the pallets are vacant. The packaging scheme efficiently uses the storage volume; the packaged volume is approximately 1.8 percent of the volume of the assembled truss.

Video Surveillance

The operator has a limited video surveillance system at the control console to monitor operations. The video system has four cameras: two facility surveillance cameras, each with pan/tilt and zoom control; and two cameras attached to the end effector, each with fixed position and focus. The surveillance cameras provide a general viewing capability with one camera located behind the robot for an over-the-shoulder view and the second camera located to the side and behind the Cartesian motion base for a panoramic view. Position and zoom control of these cameras is performed manually by the operator. The end-effector cameras provide the operator with a limited view of the mechanical components and function

as a backup for verifying sensor response. They also monitor visual lock indicators on the strut joint and provide a view of the end-effector fingers and their position with respect to the joint receptacles. The four video cameras, although helpful, do not adequately provide the operator with sufficient coverage to confirm the safe operation for the many potential collision conditions that exist during assembly; thus the cameras are inadequate for teleoperation.

Computer Control System

Assembly operations are commanded and controlled by several digital computers linked together by conventional serial communication lines. A schematic of the computer control system is shown in figure 8. The facility executive program, which controls the system coordination and operator interface functions, resides in a minicomputer workstation and uses the FORTRAN programming language. All communications are routed through the workstation; however, they could be passed directly between other processors. Data are transferred in ASCII format, which aids the development process because checkout of code for the various processors could be performed on alternate terminals and manually verified. The motion bases are controlled by a commercially available indexer board hosted on a personal computer, and the control software is written in BASIC programming language. The motion bases are capable of incremental and absolute position control. The robot arm and end-effector component commands are written in a modified version of BASIC for processing in the robot controller. The robot arm processor includes a local database, which contains arm positions and orientations required for the desired strut installation positions. This local data storage minimizes the amount of information transferred between processors. End-effector control and sensor monitoring are also performed in the robot processor because the processor has both analog and discrete input and output (I/O) capability, a feature which expedited system development. Details of the computer control system can be obtained from reference 5.

Software Design and Operator Interface

The facility executive program accomplishes supervised autonomous assembly with a specially developed modular code that can totally assemble and disassemble the truss structure. Supervised autonomy, however, requires that the operator be provided with sufficient information and interface capability to intervene when a problem arises. The modular software structure coincides with system hierarchical and mechanical functions and is shown in figure 9. The layout of the software system shown in figure 9 is composed of four basic levels: *administrative*, *assembly*, *device*, and *component*. The *administrative* level initiates the system and permits the operator to examine and modify database information and system options. Assembly-sequence files that define operations required for assembly or disassembly are created, executed, and/or modified at the administrative level. The standard operating mode is performed at the *assembly* level, and all commands for system devices, data verification, and error recovery operations occur there. To accomplish automated truss assembly and disassembly the assembly commands are successively decomposed into a sequence of *device*-level commands, which vary with the strut being installed and any special conditions that may be required for that strut. Special conditions, such as which struts have nodes preattached and which struts are connected together, are stored in a database referenced to the strut name. Also included in the database is critical information, such as the pallet number, storage position, and the current location of the strut. The location of the strut (installed in the truss, stored in the pallet, or currently in the end effector) must be updated as assembly progresses. Device-level commands are decomposed into *component* commands (lowest operational level) that control individual actuators on the various devices. For example, the component-level command "open receptacle fingers" causes the fingers on the end effector that grasp the joint receptacle to open regardless of other conditions. Sensor checking verifies the successful execution of each component command. As one works down the software program hierarchy, control and responsibility shift to the operator. At the device and the component levels, the operator must be fully cognizant of the capabilities of the hardware and the assembly operations. Consequently, all operations below the assembly level are protected by a password.

Figure 10 illustrates a typical operator display with the basic menu layout for the system, which was derived directly from the software design shown in figure 9. The boxes in figure 10(a) represent typical menus available to the operator, and figure 10(b) shows all menus and their relationship to each other. The operator controls the assembly by selecting commands from the menus displayed. The three modes of operator input are direct keyboard selection, command file, and assembly-sequence file. The keyboard input mode requires the operator to select a menu option by a direct keyboard entry. The command

file mode permits the operator to create a text file of commands as they would be entered in the direct keyboard selection mode. The assembly-sequence file is a predetermined file that executes like a command file and includes all predefined commands required to complete the truss assembly or disassembly in a particular order. The lines between the boxes in figure 10(b) indicate how the automated system or an operator traverses the various levels. The menus overlap on the screen as selections are made (fig. 10(a)) to provide an easily traced visual path. Commands being executed are highlighted so that the operator can follow the path, as well as determine the current system status. Special windows on the operator's monitor also display the name of the strut being installed and the current status of the device-level components. A message window in the display provides a running description of the component command being executed, the success or failure of the command execution, and a prompt for the operator to make a menu selection. Details of the operator control interface can be found in reference 5.

The need for a pause-and-reverse capability for error conditions that occur at sensor checkpoints was identified early in the software development phase. The implementation of the pause and reverse capability significantly affected the size and complexity of the control code. For example, the reverse command sequence does not necessarily mirror the forward sequence; therefore, special conditions and additional checks frequently had to be included in the reverse sequence. When the forward sequence was modified, the reverse sequence had to be reviewed for potential modifications. The need for an additional pause capability was identified during preliminary tests. This additional pause capability is necessary to provide the operator with total control authority at all times. Although the robot arm moves at a relatively slow rate, the operator requires the ability to interrupt the robot during any move. For example, the operator occasionally needs additional time to check between camera views or to adjust camera positions when a portion of a robot path has minimal clearance.

The path that the robot traverses is based on movement between states, which frequently are intermediate or conditional states that depend upon the installation conditions of the individual strut. When a pause is initiated by the operator, the prior state, current state, and goal state are all trapped by the computer memory. From the robot pause condition, the operator has three options available: (1) continue the path from the arbitrary interrupt point, (2) adjust the current position of the arm and continue the path from the adjusted position, and (3) reverse the path and return to the initial state. The robot motion may be paused and reversed as many times as desired, thus acting as a toggle to change the direction of motion. This capability significantly reduced the operator's level of apprehension during those maneuvers with high collision potential. The modular hierarchy of the executive control program and the operator interface menus remained virtually unchanged during the test program.

Assembly Operations

Assembly operations for the current tests were developed around traditional serial pick-and-place robotic procedures frequently used in terrestrial applications. These procedures generally rely on positioning repeatability for successful operation, and they are used in the current system for two reasons. First, many robots, including the model used for the current assembly tests, have inadequate absolute positioning capability to move to a computed global point with the accuracy required for the current assembly operations, despite the considerable number and range of passive guidance features designed into the various hardware components. Second, the end effector does not have sensors to detect range, position, and orientation of the truss joint receptacles; thus, it is unable to guide the robot to intercept them. Therefore, the installation positions of critical locations were determined and stored as taught points in the local database of the robot.

Every time a strut is selected for installation, the database is queried to determine the current status of the strut and whether the nodes to which the strut connects have been installed. If all requirements are satisfied, the installation sequence for the selected strut is initiated. The sequence begins with the robot arm at a rest position called the canister approach point, which is just above the supply canister (fig. 11). The arm first moves to a position directly above the desired strut. It then descends to grasp the strut with the end effector and removes the strut from the pallet. The arm returns to the rest position, after which the motion bases move to predefined locations. The arm then moves along a path defined by four to six taught points to the installation point. At this location, the structure is grasped by the receptacle fingers, the strut joint connectors are inserted into the receptacles, and the connectors are locked. The strut and the receptacles are both released, and the arm is returned to the canister approach point along the same path. Removal of a strut from the truss and storage in the pallet during disassembly involves essentially the reverse procedure. One of the goals in developing the assembly operations was to minimize

the number of unique operations, including the development of robot paths, required to assemble all the struts. The following subsections give a detailed account of component operations and checks performed during installation.

Installation Positions and Robot-Arm Assembly Paths

A planform view of a model of the truss is shown in figure 12. The members in the top face of the truss form two concentric hexagonal rings, which are identified by the relative positions of their perimeters as the inner ring and the outer ring. The truss is traditionally called a tetrahedral truss because it is composed of regular tetrahedrons. However, a pentahedron is a truss subelement and a typical pentahedron is illustrated in figure 12. The base of the pentahedron is a square and every member in the truss lies within the base of a pentahedron. The square base of the pentahedron provides the maximum area within the truss for access of the node for member installation. The plane of the base is referred to hereinafter as the insertion plane of the member because each member lies in the base plane of a pentahedron when it is installed.

Strut identification. A naming convention was developed for the convenience of the operator in identifying strut members. The convention includes an identifier for struts with similar orientations with respect to the physical position of the robot, and it also permits a unique identifier for any member in a large multimember truss. The convention is illustrated in figure 13, which shows a top planform view of a large planar truss of arbitrary shape. The struts in the top face are represented by lines of medium width, the struts in the bottom face are represented by lines of narrow width, and the core struts are represented by dashed lines.

A node in the top surface is arbitrarily selected as the truss reference node. For the test model, the truss reference node is at the center of the rotational motion base. The wide solid lines outline n concentric hexagonal rings with the center at the reference node. The ring number is the first identifying parameter; four rings are outlined in figure 13(a). Each ring is subdivided into hexagonal cells, the boundaries of which are formed by the dashed lines of the core struts. The cells are denoted in the figure by the numbers within the ring. Each ring includes $6(n-1)+3$ cell units, and each cell is composed of 12 individual struts. The cell is the basic repeating unit in the truss and was the element used for development of assembly operations. The individual struts in each cell are denoted by the location of their nodes that lie on the even number positions of a conventional clock face. The labeled nodes of a typical cell are shown in figure 13(b). Each strut in the truss is identified from the perspective of the operator by the ring number (R), the cell number (C), and the clock node positions. A typical strut in the top face is labeled in the figure as R2,C2,8_4. This convention provides a unique designation for all struts in the top and bottom faces. However, each core strut lies on a cell boundary; therefore, it can be identified by either of its two cell designations.

The cell nodes shown in figure 13 at clock positions 12, 4, and 8 are always in the top face, and those at clock positions 2, 6, and 10 are always in the bottom face. In identifying a member, the node at the 12 o'clock position is used as the individual cell index node; this node is always in the top face of the truss. An individual cell has 120° rotational symmetry about the geometric center; therefore, as the truss is rotated about the reference node, the index node of an individual cell will change. For example, as the truss in figure 13 is rotated about the reference node, the index node of ring 1 cell 1 moves to the 8 o'clock position at 120° and to the 4 o'clock position at −120°. Although the index node for that cell changes, the orientation of the 12 struts is preserved. An examination of the truss cell in figure 13(b) indicates that the structure has 120° rotational symmetry about the reference node. The geometric pattern evident at 0° is the same as that at ±120°, and the pattern evident at 180° is the same as that at ±60°. Therefore, local position and orientation, as well as general position and orientation of the members, are preserved by rotations of 120° increments. This repetitive pattern enables many struts to be installed by teaching a few basic installation paths in a reference cell. The same installation paths are used for struts in adjacent cells by changing the location of the rotational motion base or by repositioning the robot via the Cartesian motion bases.

Robot assembly paths. The individual strut installation positions are illustrated in figure 14. A typical unit cell, such as the one shown in figure 13, is identified in figure 14 as cell A. Each unit cell has three pentahedral base planes; the normals to the base planes are orthogonal. The installation position is at the center of the strut and the direction of insertion is indicated by the arrow on the figure. The insertion directions are restricted because the mouth of the joint receptacle only permits entry in one direction (see receptacle in fig. 3), although the end effector could approach the receptacle in the insertion

plane from either direction. All members in both the top and bottom faces are installed with x'-axis of the end effector directed away from the center of the cell, and a unique path is required for installation of each of the six face struts. The receptacles of the core struts are oriented to provide a rotational symmetry about the node. This convention was adopted so that all nodes would have receptacles aligned in the same direction. Because of the rotational symmetry and planar alignment, only three robot paths are required to install the 6 core struts. Therefore, a total of nine robot installation paths must be taught for the 12 struts in cell A.

The entire truss could not be assembled by using only the nine paths previously noted because of the limited reach of the robot arm. Some struts in the second ring required that the rotating motion base be aligned at intermediate 60° increments. An examination of a typical cell, such as cell B in figure 14, from a viewing angle of 60° indicates that the node nominally in the 12 o'clock position is located in the bottom face of the truss. Therefore, the index node for any cell at 60°, −60°, and 180°, as observed by the operator, is rotated 180° to lie in the top face; these cells are hereinafter referred to as inverted cells. The struts in inverted cells have insertion planes that are rotated 90° when compared with similar planes in cell A, and the insertion directions of the core struts are opposite of those in cell A. The truss assembly required six robot paths to be taught in the inverted unit cell.

In addition to the nine installation points in the normal cell and six points in the inverted cell, four additional installation paths had to be taught. The additional paths were required because 28 core struts had nodes preattached. The storage configuration shown in figure 7 dictated that these nodes should be located on specific ends, which in some cases were different from the end dictated by the normal path for that strut. Therefore, these core struts had to be rotated end for end after they were removed from the pallet. The paths followed by these core struts are referred to as flipped paths. A total of 19 installation paths was required for complete assembly of the 102-strut truss.

The installation point at the end of the path is the most critical point because it requires accurate positioning. These points were defined by selecting a motion-base position for the robot and then stationing an observer near the truss to guide the operator who maneuvered the robot to a location where the fingers of the end effector could be closed on the joint receptacle vee grooves. At this arm position, the tare on the load cell associated with the end-effector mass was set to zero before the structure was grasped. Loads associated with misalignment were used to reposition the arm; the final position and orientation were stored (taught) as the installation point for all struts with that designation. Other points along the path were also stored as a series of Cartesian coordinates in the local database of the robot. All paths are traversed by following these points in a sequential order with the robot control system. Many paths contain common points because the actual location of the arm is not important as long as the end effector does not collide with previously installed struts.

Typical installation paths are illustrated in figure 15 by sketches that depict the paths for struts 10_2 (fig. 15(a)), 12_2 (fig. 15(b)), and 6_4 (fig. 15(c)) and a photograph of the end effector approaching the installation point for strut 6_2 (fig. 15(d)). The figure depicts the location of the strut in relation to struts that have been previously installed. The core struts in figure 15(a) to 15(c) are shown as dashed lines, and the struts in the top and the bottom faces are depicted as solid members. The figure shows the relative location of the motion base, the viewing angle with respect to the truss cell, and the location of the strut being installed from the top view. Although the arm path always begins at the canister rest position, the arm is generally moved first to a point that places the end effector in front of the robot or above the robot shoulder. The paths in the sketches are depicted by a sequence of lines from the end effector in front of the robot. Some of the paths, such as those for struts 10_2 (fig. 15(a)) and 12_2 (fig. 15(b)), are simple and were easy to develop because the region in the vicinity of the installation point is uncluttered. Other paths, like those for strut 6_4 (fig. 15(c)) and strut 6_2 (fig. 15(d)), were complex.

Several observations can be made from an examination of the photograph in figure 15(d): (1) the left side of the end effector is aligned with strut 12_2 and must move along it to reach the installation point; (2) the end effector must be maneuvered within the interior of the cell close to adjacent struts and the potential for collision is high, especially near the node receptacle; (3) the region in the vicinity of the node is congested and the short length of the joint, which is desirable for structural purposes, requires all mechanical components on the end effector to be located near the node; (4) the strut installation position is near the reach limit of the robot because previously installed struts must be accommodated; (5) the robot has a relatively long forearm that limits the dexterity and frequently causes the arm to be operated near the pitch and yaw limits; (6) the storage canister

may interfere with the capability to position the motion bases for the development of paths; and (7) path and sequence planning must be coordinated, because struts 10_8, 8_6, 12_8, or 8_4 in this cell cannot be installed before strut 6_2 because they will block the path. The path used to install each strut is also used to return the arm back to the rest position; therefore, the path cannot violate the space of the strut that it is installing. Every path was traversed by using only the 6 DOF robot arm; none involved the 9 DOF coordinated motion of the robot and motion bases.

Strut installation cases. Three strut installation cases were established by connectivity conditions: direct, capture, and pyramid completion. Direct installation is the most straight forward and requires that the joint connectors be inserted into receptacles that are structurally affixed to other struts in the truss. For this case, the strut is moved directly to the installation point. Some struts are installed between fixed nodes, and others with a node preattached are installed at one end to a fixed node. For struts that have nodes preattached, the end effector operates only the mechanisms on the end being installed and leaves the strut and node combination cantilevered. Because the tests were conducted in a $1g$ laboratory without gravity compensation (where g denotes acceleration due to gravity; that is, $1g \approx 9.81$ m/sec^2), the mass of the node caused the strut to deflect from the installed position. To minimize the gravity-imposed deformations, only core struts were installed in this manner.

The cantilevered core strut creates the second strut installation case, that is, capture installation. For this case, the end effector is required to install a strut between a fixed node and the free end of a cantilevered strut that is deflected by gravity. For this case, the end effector is moved along the installation path to the approach point, which is about 10 cm in front of the installation point. From the approach point, one end of the end effector is moved to the deflected node of the cantilevered strut and the fingers are closed, thus capturing the receptacle. After capturing the deflected receptacle, the end effector is moved to the installation point. At the installation point, the strut is inserted into both node receptacles and the joints are locked. This procedure was adopted because the deflection of the cantilevered struts was repeatable within the capture envelope of the end-effector fingers. The capture and movement of gravity-deflected struts to their installation position made the assembly task performed in these tests more difficult than the installation positioning required for space assembly, because any displacements encountered in $0g$ should be significantly smaller than those encountered in $1g$.

The third strut installation case, pyramid completion, is similar to the capture installation case except the captured node receptacle is connected to two cantilevered struts and the gravity-induced deflections are not as large. The robot moves for the pyramid-completion sequence are similar to those of the capture sequence; however, the direction of displacement of the two connected struts is restricted to the normal to the plane formed by them. When the strut in the pyramid-completion sequence is installed, a substructural pyramid or a stable frame is completed.

Strut Assembly Sequence

The sequence in which the struts are assembled is illustrated in figure 16 and the rules that govern the development for this test series are listed in the appendix. The wide lines in figure 16 indicate the ring boundaries, and the numerals in the center of the hexagonal cells designate the cell numbers. The numbers outside the perimeter of the second ring represent cell numbers for the third ring, which are required to identify six of the struts on the boundary. The small numbers adjacent to each strut represent the sequence in which the members are installed. The three nodes in the center of the bottom face are preattached to the rotational motion base. These nodes are fixed and used as anchor points for stabilizing the assembled members. The first six struts installed compose the center tetrahedron that, supported by the three anchor points, serves as the initial structural unit. Struts with nodes lying in the top face are then added around the perimeter to form the first ring. The second ring is assembled circumferentially in two parts. Those core struts that connect the top nodes of the first ring to the lower nodes of the second ring and the struts that interconnect the lower nodes of the second ring are installed first. The core struts that connect the upper and lower nodes of the second ring and the interconnecting struts in the top face of the second ring are installed to complete the process. The rules governing the development of the sequence (see appendix) do not overconstrain the selection of struts so that there is only one option available as the sequence progresses. Coordination of the assembly sequence with the availability of struts in the pallets, however, significantly reduces the available options. Generally, several potential strut candidates are available at each step, and the choice, in many cases, is arbitrary.

Force and Torque Position Control

During strut acquisition from a pallet and installation in the truss, the end effector is coupled between two structurally stiff components: (1) the robot arm, and (2) the struts that are restrained by pallets or by the receptacles attached to the truss nodes. A small error in positioning by the robot or the motion bases will induce large loads in the end effector that may cause the mechanical components to bind, and result in a command failure. The positioning repeatability reported by the robot manufacturer (0.01 cm) and the repeatability measured on the motion bases (approximately 0.02 cm, according to ref. 3) are high; however, they do not take into account all conditions, many of which are difficult to control. For example, the base frames of the X and Y motion bases are aluminum and variations in temperature can result in significant deformations; the external temperature changes to the robot, as well as heating of the robot motors, can affect robot repeatability; the truss members have small length errors; and modifications to the end effector cause changes in the mass and/or mass distribution. All of these size variations affect the position and orientation of taught points. The forces and torques produced by position displacements, which were measured by the load cell located between the robot wrist and the end effector, were used to direct robot repositioning. Commanded translation and rotation moves to reduce the loads were based on the following linear relation:

$$\text{Position adjustment} = \frac{\text{Load} - \text{Bias load}}{\text{Stiffness constant}}$$

The stiffness constants for the force axes were determined empirically and were assumed to be the same along all three translation axes. The stiffness constants for the three moment axes were also empirically determined, but they were different, primarily because of the length of the end effector. Bias loads were used in conditions in which changing the tare is desirable. For example, to remove a strut from the pallet, the end effector is moved toward the strut until the force exerted on the end effector is 89 N. This empirically determined condition ensures that the end-effector latches would be forced closed and the strut would be captured when the latches were commanded to be locked.

The load cell is nulled to remove the mass of the end effector at the operating orientation before making contact with a strut or pallet. To reposition the robot arm after contact, the force-torque control algorithm computes the three translations and three rotations based on the linear relationship, and the arm is commanded to move to this location. The loads at the new position are then obtained and the cycle is repeated. If the load and torque measured along any axis is less than a specified deadband value, that load is ignored. Also, limits are imposed on each commanded displacement and rotation. Deadband and limit values were empirically established as the following: deadband force, 3.6 N; deadband moment, 0.57 N-m; displacement limit, 0.025 cm; and rotation limit, 0.01°. The positioning control algorithm is cycled until one of the following terminating conditions is satisfied: (1) all six components are simultaneously within their respective deadband values, (2) the algorithm has cycled through 30 iterations, (3) an external signal from another component indicates that an event has occurred that eliminated the need for additional positioning control. Terminating condition 3 may occur when a strut is being acquired from a pallet and microswitches on the strut holder indicate that the spring-loaded latches are closed. Force and torque position control is routinely incorporated in all installation and removal sequences that require the end effector to contact or be coupled to a constrained component. The passive guidance features on the end effector, the strut receptacle, and the alignment adapter are instrumental in guiding the robot arm to a position where the loads along all axes are within the deadband. Final positioning displacements for reliable operation of the end effector were approximately 0.005 cm.

Strut Pallet Operations

Strut acquisition is initiated with the end effector at the canister approach point, at which the receptacle fingers are closed to prevent collisions with adjacent struts in the pallet and the force-torque load cell is nulled. Each strut has an assigned pallet and slot number stored in the database. To acquire a strut, the end effector is moved in a horizontal plane to a location immediately above the strut and then vertically down to a point arbitrarily selected to be 6.4 cm above the strut. This point, which is referred to as the canister grasp point, is a relative point and is computed as an offset to the canister approach point. This technique minimized the database storage and reduced the time and effort required to teach each of the 102 individual strut locations. At the canister grasp point, the end-effector platform is extended, and the receptacle fingers are opened on the end with any preattached node. The end effector is then moved vertically toward the strut to a point where the strut grippers should begin to make initial contact, and control is

transferred to the force-torque position-control algorithm. The robot moves the end effector incrementally toward the strut along the x'-axis and the force-torque algorithm adjusts the y'- and z'-positions as required to minimize the loads along these axes. Movement toward the strut continues until the load cell indicates an x'-axis bias load of 89 N or the microswitches on the strut latches indicate they have closed. When either of these conditions is satisfied, the strut latches are commanded to close. The robot is again repositioned to remove all forces and torques (including the 89-N bias load) and to eliminate any binding that may occur between the strut and pallet that could cause the pallet to be lifted as the strut is removed. The platform is then retracted and the strut carried to the canister approach point where the fingers are opened in preparation for installation.

Motion-Base Moves

The installation of each strut requires that the base of the robot be at a particular location with respect to the assembled position of the strut in the structure; consequently, there is a set of motion-base positions for the installation of each strut. A simple positioning algorithm was developed to reposition the motion bases so that the robot arm would not collide with any of the struts previously assembled. This algorithm requires that the current motion-base positions, the required motion-base positions, and the geometry of the currently assembled struts be computed and checked for potential collisions. Motion-base moves are sequenced to avoid collisions and, in some cases, additional collision avoidance moves are required. All moves are made with the robot arm in the rest position (canister approach point) to minimize the distance the arm extends toward the truss. The collision avoidance algorithm is described in reference 5.

Strut Installation

A strut is inserted in the truss by moving the end effector to the location where the receptacle fingers are over the vee groove notch of the joint receptacle, as shown in figure 5. The fingers are closed in the vee notch and clamp onto the receptacles with minimal free play. When the fingers are in the closed position, the cam drive mechanism does not permit them to be forced open. If the end effector is misaligned, the fingers are designed to capture the receptacle at any location within a 2.5-cm-radius by 1.4-cm-long cylindrical envelope and to guide the end effector by force-torque control to a location suitable for installation. The strut connector plunger is pushed into the receptacle while the fingers grasp the receptacles.

The platform is held at the installation position while a small gear-head motor rotates the locking nut to secure the joint. The locking nut is turned until one of the following events occurs: (1) the motor current reaches a value that corresponds to a predefined torque associated with a locked joint, (2) the number of motor rotations exceeds a predefined nominal value, or (3) a predefined time limit is exceeded. If either event (2) or (3) occurs, or the number of motor turns is less than a predefined value, the operator is alerted for a potential error. After the joint is successfully locked, the strut latches are released, the platform is retracted, the receptacle fingers are opened, and the end effector is moved back to the rest position via the installation path.

Pallet Transfer Operations

The pallet pickup procedure is similar to the strut acquisition procedure; the same end-effector latch mechanisms and software routines are used. The locations of the pallets in both the supply and storage canisters are calculated as offsets from taught points. The pallets traverse the canister against nylon guides at the corner posts. To store a pallet, the strut latches are commanded to open slightly above the store position, then the arm is commanded to move down in increments until a force of 156 N is applied to the pallet handles. These commands force the pallet into a set of spring-loaded pins, which hold it in place.

Error Recovery

If a sensor detects that an actuator command is not successful, the executive program pauses the system and notifies the operator by displaying a menu with potential corrective commands. The operator repositions the video cameras with the manual pan, tilt, and zoom features to determine the current physical situation, and then selects a command from the menu. The sensor is checked again at the completion of the selected command. If the condition that initiated the pause is not corrected, the error menu is again displayed so that another command may be selected. The operator may choose to ignore the condition and proceed. If the condition is ignored, the anomaly is considered to be of little consequence. When the sensor check indicates that the condition is resolved, the automated system resumes operation at the step following the one where the pause occurred. If a local problem cannot be resolved, the operator may reverse the operation and return the

system to the initial state. This capability relieves the operator of having to recall detailed sequences of component level commands and manually backtracking to the initial state. An assembly error is recorded when a failed actuator command is followed by an operator initiated command that changes the normal installation sequence or the robot position. An operator initiated pause followed by direct component commands, rather than a normal return to the automated sequence, is also considered an error. If a pause condition is associated with the hardware and the operator is unsuccessful in resolving it from the console, the last resort is to enter the assembly area with the robot disabled and manually intervene.

Tests, Data Acquisition, and Analysis

A total of four end-to-end assembly sequences, each followed by an end-to-end disassembly sequence, have been conducted. The first two assembly sequences were preliminary tests that resulted in a number of minor hardware and software modifications. The last two sequences have been analyzed to establish a set of baseline results by (1) examining the time required to perform each assembly task that relies on traditional robotic techniques, (2) examining the reliability of the system to determine if the mechanical and software concepts implemented are suitable for space applications, and (3) evaluating the effectiveness of the commands available to the operator to resolve all error conditions with the available video coverage and available menu options.

Each assembly test is initiated with the three support nodes attached to the rotational motion base and all struts arranged in the pallets stacked in the supply canister. The robot and the motion bases are commanded to predefined positions by the operator to verify their calibration. After all calibrations have been verified, the operator initiated the assembly sequence. Timing for strut installation begins with the robot arm at the rest position above the strut canister. Seven time segments are recorded in the sequence that was previously discussed and illustrated in figure 11. The first segment times the robot as it moves the end effector to the acquire position immediately above the desired strut in the canister. The second segment times the following: (1) force-torque controlled repositioning of the end effector at the strut acquisition point, (2) locking the end-effector latches, (3) repositioning the arm again, and (4) retracting the platform. The third segment times the return of the end effector to the rest position. The fourth segment times the movement of the motion bases to their predefined locations, which includes collision avoidance maneuvers. The fifth segment times the robot arm as it moves along the preplanned path to the installation point. The sixth segment times the following: (1) force-torque controlled repositioning after closure of the fingers, (2) strut insertion, and (3) joint locking. The seventh segment times the arm during moves along the return path to the rest position. Several of these segments might appear to be similar for all struts (e.g., arm motion from the rest position to the installation point and the return (segments 3 and 7)). However, the intermediate moves required to capture the receptacles of the cantilevered members make the times for these segments different.

The automated tests followed the manually developed strut assembly sequence stored in a predefined command file. The entire assembly operation, including transfer of empty pallets to the storage canister, is automated. Data for assembly time and error recovery are recorded by the operator with a personal computer spread sheet program. The operator records the time of each segment of the sequence and each error with single keystroke commands. The operator also records the type of error and the recovery options employed. Following the tests, the data were analyzed to determine the time for the various strut installation segments and the variation in time for struts with identical installation conditions. Errors were examined to identify systematic problems that may be associated with operational procedures, hardware failures, or errors in taught points. Recovery options were examined to identify those problems that may be resolved by an automated routine or minimized by additional sensors and/or hardware and software improvements. To avoid operator fatigue, all tests were performed in time blocks of 4 to 6 hr, instead of a continuous start-to-finish operation.

Results and Discussion

Assembly Time Results

The total time required to acquire and install each strut during assembly and to remove and store each strut during disassembly is shown for each test in figure 17. The assembly proceeds in ascending order by strut number and disassembly proceeds by descending order. The total time, indicated by the height of each bar, includes all seven time segments, but it does not include the time to assess and correct errors. The various error conditions and the time required to assess and correct them will be discussed later. The average time required to install a strut is slightly over 9 min and the average time to remove a strut is slightly below 9 min. These averages were obtained by summing the total time for

each strut and dividing by the number of struts successfully installed or removed. The installation and removal times for both tests ranged from a low of about 7 min per strut to a high of about 12 min per strut. The 5 min range of assembly times occurs because of the following factors: (1) some struts required one or more of the motion bases to be moved and others required no motion-base moves, (2) some struts that required motion-base moves also required extra moves to satisfy collision avoidance conditions, (3) the length and the complexity of the path and the speed of the robot in traversing the path segments from the canister approach point to the installation point were different for the various struts, (4) the installation path for struts that connect to cantilevered members required intermediate moves and end-effector operations to capture the receptacle and place it at the installation location, and (5) the amount of time required for force-torque repositioning (at 1 sec per cycle) varied from a few seconds to as much as 2 min.

The operational time for both installation and removal of any given strut is generally repeatable (within about 1 min) from test A to test B. Fourteen struts in the assembly test and 21 struts in the disassembly test have a variation between the tests greater than 1 min. This variation is due primarily to (1) the number of cycles required by the force-torque algorithm to reposition the end effector and (2) upgrading the collision avoidance algorithm between tests A and B. The data indicate that, in most cases, the difference in motion-base time is responsible for the variation in time between assembly tests A and B. The standard deviation (σ) was computed from the data for each test and is shown in figure 17. The standard deviation for each of the tests is slightly over 1 min. The results for struts 31 and 43 in assembly test A, strut 94 in assembly test B, and strut 29 in disassembly test B were not included in the figure because an error condition occurred during their installation and removal that required manual intervention.

The time to install any specific strut is generally different from the time required to remove the strut. This difference occurs because moves of the motion bases for assembly may be different from those required for disassembly. Also, the assembly time includes one more force-torque repositioning cycle than the disassembly time. Because the effects of force-torque repositioning and motion-base moves have the potential to significantly vary the test results shown in figure 17, the times required for these two segments were subtracted and these results are presented in figure 18. The average time for the two deleted time segments was slightly over 2 min for each test set. The standard deviations indicated in figure 18 for both the assembly and disassembly tests are significantly reduced from those in figure 17. About 80 percent of the times for both the assembly and disassembly tests are within ± 1 standard deviation. The time for struts with differences exceeding ± 1 standard deviation were examined and the data indicated that a higher than normal end-effector mechanism time (segments 2 and 6) was recorded in one of the tests. The reason for this difference, however, could not be determined from the data.

The remaining source of variation in time between struts within a test set was the effect of the path. The time required for installation and removal of struts in positions 6_2, 8_4, 10_8, and 12_8 are shown in the bar graphs in figure 19. These particular paths were selected because they represent various installation conditions, several levels of path complexity, and each path is used at least six times during a test. The results were similar to those shown in figure 18 because they do not include the time for force-torque repositioning and motion-base moves. Note that the installation and removal times are generally the same for a given path condition. The 6_2 path with capture installation condition generally requires more time than the other paths illustrated. The results are generally consistent, although the standard deviation is higher than might be anticipated with those segments that have the highest identifiable variation removed. The remaining differences may result from operator-initiated timing anomalies; however, the exact cause could not be determined.

The total time for each segment of the assembly and disassembly sequence was summed for all struts successfully installed and removed; the results are presented in figure 20. The time for the segments in the individual tests as well as the averages for both tests are shown at the top of the figure. The percentages are illustrated in the pie chart at the bottom of the figure. Evaluation of the results on this basis permits the various segments to be examined by their relative size for the total operation. Although there are relatively large variations in the times of individual struts, as discussed previously, the total times for the various segments were repeatable. The largest variation for the assembly test was just over 5 percent and occurred in segments A, C, and F. Several of the segments in the disassembly tests had larger variations, with the two largest occurring in segments H and N. However, segments H and N are small; therefore, this larger variation did not significantly affect the total time.

The largest time increments associated with acquiring the strut from the pallet and installing the strut in the truss are B and F, as indicated on the pie chart of figure 20. Both operations involve significant time for force-torque repositioning which is slow in the current system because the algorithm is performed iteratively outside the robot control system and the range of moves is limited as a safety precaution. Each force-torque repositioning iteration typically requires about 1 sec to perform; the data indicates that 1 to 2 min were frequently required to reduce the loads to within the deadband values. The input and output for actuators and sensors on the end effector are controlled by an analog system that is a part of the robot electronics. Simple end-effector operations like acquiring a strut by the end effector (and removal from the end effector) typically involve several actuator and sensor checks, each of which require approximately 1 sec to perform. The time for both actuator and sensor verification and force-torque repositioning could be significantly reduced by placing the force-torque repositioning under the command of the robot controller, and the end effector under the command of a dedicated microprocessor.

Robot arm movements to transport the end effector from the rest position to the installation point and return require about 30 percent of the approximate 9 min assembly time for each strut and involve robot arm speeds from 5 to 18 cm/sec. Higher robot arm translational speeds were initially considered; however, the operator indicated that higher robot speeds were not desirable because the end effector was occasionally within 2 to 3 cm of installed struts. The operator must have time to intervene to prevent collisions, and there were several locations along installation and removal paths where the robot must move in close proximity to installed struts or fixed components. Not only is reaction time critical, but the operator must be comfortable with the operating speed so that stress is minimal.

Estimated Time for Assembly in Space

The results of the tests reported herein were examined to estimate the time required for assembly of the system in space. The average strut installation time in figure 20 was adjusted for differences that could occur during assembly in space and the resulting projection rounded to 0.10 min is illustrated in figure 21. The time increment for segments B, D, and F are estimates based on anticipated technology developments. For example, an in-space system is anticipated to have two major characteristics that will significantly affect installation time that are not included in the current system. First, an in-space system is anticipated to have active compliance provided by force-torque feedback in the robot control loop. This feedback will eliminate the lengthy force-torque repositioning sequences included in time segments B and F. Therefore, the robot repositioning times included in the results shown in figure 20 were eliminated from time segments B and F in figure 21. Second, an in-space system is anticipated to have a distributed computational architecture controlled by an executive scheduler that will permit parallel operations to occur. Parallel operations will permit the motion bases to reposition the truss and move the robot to the required position while the strut is being acquired from the pallet. Therefore, the time for segment D in figure 20 was eliminated from the estimated time for an in-space system in figure 21. These changes result in an anticipated average strut installation time of 4.4 to 5.4 min for an in-space assembly system. This installation time is slightly over half of that required for installation in the current system.

Comparison With Simulated EVA Assembly Results

The assembly times projected from the tests reported herein were compared with those times for manned assembly tests performed in a neutral buoyancy simulation and reported in reference 6. The neutral buoyancy tests used similar size test hardware, but the truss joints were designed for rapid assembly by astronauts; therefore, the joint locking mechanism was different. In the neutral buoyancy tests, a section of a tetrahedral truss consisting of 12 nodes and 31 struts was assembled by two pressure-suited test subjects. In the two assembly tests that were conducted, the average time to install the struts was slightly under 0.7 min per strut. This time was considerably less than either the approximately 9 min required for assembly in the investigation reported herein or the projected fastest time of 4.4 min for an automated system in space (fig. 21). The factors effecting the difference in the time required for the two tests are as follows: (1) the paths used by an astronaut for acquiring and positioning struts easily conform to the existing structure and collisions are less likely to be catastrophic; therefore, the path is shorter and the translation speeds may be much higher than those of a machine controlled system; (2) the end effector requires time to command actuators and check sensors; and (3) the end-effector must grasp struts at a specific location to maintain position and alignment.

Rapid assembly time is critical for astronauts because the time available for EVA is limited. Speed

is much less significant for an automated system because it can operate continuously for long periods and be monitored in shifts from Earth. Although the time required to assemble truss structures with a space-qualified system is anticipated to be about one-half the time required in the current laboratory tests, it may never be as rapid as the assembly done by astronauts during an EVA. Also, neither the test performed in the current investigation nor the test reported in reference 7 present the total time for construction. Tasks such as transfer of materials and equipment to the worksite, or optimization of the procedure were not considered. Although comparisons of time for humans and machines to perform similar operations are frequently made, they are of little value without examining broader aspects, such as the total time to complete all tasks. The overriding consideration for an automated assembly system is the capability to complete all tasks and handle error conditions without the need for EVA. The most critical indicator of success, therefore, is the capability of the operator to resolve all error conditions from the console.

Error Conditions and Resolution

A number of error conditions were encountered during the tests reported herein. The struts and the time required to identify and correct the errors for each strut are shown in figure 22. For assembly test A, 70 errors occurred during the installation of 59 struts. For assembly test B, 52 errors occurred during the installation of 41 struts. Each error condition required an average of 2 min to correct. Most errors occurred when the end effector was positioned at the truss during installation; none occurred while acquiring the strut from the canister. The errors associated with positioning the end effector at the truss generally caused the fingers on the end effector to completely miss the vee groove on the joint receptacle or prevented the platform from fully extending during insertion of the joint connector into the receptacle. The error sources that caused the fingers to miss the vee groove on the joint receptacle are as follows. First, the robot arm would occasionally lose calibration and would go to a stable position with the forearm rolled several degrees from the calibrate position. After this event, the taught points of the robot arm would misorient the end effector by several degrees, and predicting when and why this error would occur was difficult. This problem would not be expected to occur with a space-qualified robot arm. Second, although the robot arm was stiff, differences in mass of the end effector with different strut conditions cause changes in end-effector positioning. To minimize the number of taught points, this condition was not accounted for. Third, although the deflection of the cantilevered core struts was generally repeatable, the core struts on the truss perimeter did not have a full compliment of receptacles. Therefore, they did not have a mass as large as that of the interior nodes which had a full compliment of nine attached receptacles.

Analysis of the data indicates that during assembly tests A and B, the operator was required to correct positioning errors for over half the struts installed in the capture and pyramid completion cases. The variations in cantilever-deflected position due to mass and thermally induced expansion errors in the robot and motion-base system likely account for all the positioning errors. The $1g$ laboratory environment without gravity compensation made using traditional robotic procedures challenging. The errors that caused the fingers to miss the vee groove were corrected by the operator with a position adjust routine that commands the arm to move incrementally along the end-effector coordinate axes.

The errors associated with failure to fully extend the end-effector platform were caused by the shoulder of the receptacle hitting the connector and blocking entry of the connector plunger. These errors occurred primarily during the installation of struts that were cantilevered after installation and during installation of struts to those cantilevered struts. These errors were resolved by the operator with the position adjust routine. However, in future tests they could be effectively resolved by improving the passive guidance features of the truss joint and stiffening the side support of the end-effector fingers. The passive guidance ramps at the entrance to the receptacle are at angles too shallow to be effective. In conducting tests of this type, the total set of operations should be repeated often enough to ensure that the operator encounters nearly all possible problems. The frequent occurrence of a problem type provides insight into design modifications that should be implemented.

As indicated in figure 22, fewer errors were encountered during disassembly of the truss than were encountered during assembly, especially for test A. Most errors with the disassembly sequence were similar to those that occurred during the assembly sequence, and the majority were associated with positioning the end effector at the truss. The disassembly requires fewer struts to be captured in displaced positions. Unlike the assembly sequence, however, several errors did occur at the canister while placing the struts in the pallet slots. These errors occurred because the alignment of the strut with the pallet slot is

more critical in a store sequence than the alignment of the end effector with the strut in an acquire sequence. Overall, offsets to a single taught point for operations in the canister were more successful than multiple taught points for strut installation and removal at the truss. (The canister was at a fixed position on the Y-axis motion base and there are fewer potential sources of positioning error.) The data in figure 22 indicate that more errors occurred during test B disassembly than during test A disassembly. A review of the results indicate that the error increase is likely due to a decreased attention to robot arm calibration during test B disassembly.

Although the operator successfully corrected position errors and effectively performed the truss assembly, the reliance on taught points for close positioning is not adequate for space operations. Simulating all cases of $0g$ positioning in a terrestrial based laboratory, as well as the thermal conditions that can affect positioning requirements, would be too difficult to teach points accurately enough for in-space assembly. These difficulties highlight the need for a sensor system mounted on the end effector with the capability to detect both position and range of the receptacles and an algorithm to guide the arm to the installation point. As a result of the tests reported herein, considerable work has been done to develop a machine vision capability for assembly of the current truss. Preliminary tests conducted on the machine vision system can be found in reference 7.

Twice during assembly A and once during assembly B, manual intervention was required for similar conditions. The entry of the strut joint into the receptacle was blocked because the connector did not have adequate passive guidance. The truss is a redundant structure, however, small errors in member lengths can accumulate to cause internal loads and errors in the position of the receptacles. Studies have been conducted on the effect of member length errors on the position and internal loads in truss structures and are reported in reference 8. The potential for this condition was known during the design; consequently, passive guidance features were incorporated in the receptacle and connector. However, the angles were too shallow and they were not as effective as anticipated. The fingers and their supporting structure were not adequate to provide the necessary stiffness for positioning. The fingers were designed primarily to position receptacles that were attached to cantilever-supported struts.

Test Observations

All tests, including the two preliminary assembly and disassembly tests, were performed by the same operator. The preliminary tests permitted the operator to gain experience and become proficient in using the menus for error diagnosis and resolution. The success of the operator in using the menus to correct the errors from the console is very encouraging for the future development of in-space assembly systems. The tests did indicate, however, that all assembly and disassembly operations must be under automated computer control with built-in checks and limits. It is difficult for even a highly experienced operator to remember all the steps and checks involved in a segment of the assembly sequence. All manual commands in an in-space operating system should be verified by on-line knowledge based tools to ascertain advisability and safety before execution. The capability to pause the system at any time to survey conditions and verify a particular sequence or the operation of a sensor proved to be essential.

The operator was able to successfully monitor most end-effector operations with the limited video coverage and command adjustments on the hardware components with a few visual enhancements. Visual markings that assist the operator in determining the direction and amount of adjustment required for manually controlled repositioning are critical. However, video coverage was not adequate to evaluate potential collision conditions between the end effector and many previously installed struts.

The concept of the end effector grappling the strut receptacle to assist in inserting a strut was operationally essential. Alternative techniques such as using the robot arm to push the strut directly into the receptacle were considered in the development, but they were abandoned for the current approach because misalignment could not have been compensated for by repositioning because no reference position would be available. Also full instrumentation of the end effector was critical to confirm the success of each command, and to provide the operator with status information. The operations and sensor checks performed on the end effector during strut acquisition and installation for the current system are very basic, although they involve approximately 33 command and check operations.

The assembly and disassembly tests conducted were successful in identifying potential problem areas, many of which would not have been readily anticipated or incurred through simulation studies. Addressing the total integrated task, instead of independent bench testing of component parts, forced all aspects of the task to be evaluated. A significant portion of the system capability has been empirically developed and a larger number of installation conditions were accounted for in this terrestrial-based test

than would be required for an automated system operating in $0g$. Although the current test results indicate that additional developments in specific areas need to be examined, automated in-space assembly of large truss structures for precision antennas is a desirable and viable construction method.

Concluding Remarks

A number of proposed space missions include precision reflectors that are larger in diameter than any current or proposed launch vehicle. Most of these reflectors will require a truss to accurately position the reflector panels, and these truss structures typically incorporate hundreds of struts. Member-by-member installation using special robotic manipulators, controlled by a supervised autonomous system, appears to offer significant potential for assembly of these trusses in space. A research program has been conducted to develop the technology required for an automated system capable of performing the required assembly tasks. The focus of this research has been on the hardware concepts, the software control system, and the operator interfaces that are necessary to reliably perform the assembly tasks and handle error conditions. A special facility was constructed and several assembly tests of a 102-strut tetrahedral truss were conducted.

A set of baseline tests were conducted around traditional "pick and place" robotic procedures, which are frequently used in industrial applications. These traditional procedures generally rely on the positioning repeatability of all movable components for successful operation. They were used in the baseline tests because many robots have inadequate absolute positioning capability to move to a computed global location with the required accuracy for the assembly task. Four end-to-end assembly sequences of the truss were conducted, each followed by an end-to-end disassembly sequence. The first two sequence sets were preliminary tests resulting in a number of minor hardware and software modifications. The latter two sequence sets were analyzed to establish time lines against which future tests that may incorporate modifications can be compared. All automated operations in the tests were controlled by predefined sequences stored in a command file. The operator intervened only when the system paused because of the failure of a sensor to receive the proper response to an actuator command. An error was considered to occur when the operator was required to initiate direct component commands from the console to resolve the condition that initiated the pause, rather than to continue the normal sequence.

The time needed to acquire each strut from a supply pallet and install it in the truss during assembly, as well as to remove a strut from the truss and store it in a pallet during disassembly, was recorded for each of the 102 strut members. The average time required to perform the assembly and disassembly operations was approximately 9 min per strut. The variation for individual struts within the tests is about 5 min because some struts required the base of the robot to be repositioned prior to the installation; the distance, complexity, and speed of the robot in traversing the path from the canister to the installation position differed for various struts; and final end-effector positioning required force and torque controlled realignment, which varied from a few seconds to 2 min. The time for assembly of any given strut from one test to the next was generally repeatable within 1 min.

The test results were used to estimate the strut installation time for assembly of the truss in space, and 4.4 to 5.4 min per strut can be expected. This estimate is contingent on anticipated improvements that include the use of a dedicated microprocessor to initiate the sequence of actuator commands and verify their success via sensor checks, the force and torque controlled repositioning of the end effector being performed within the robot control loop, and the simultaneous movement of some components controlled by an executive scheduler. The ability of the operator to intervene should a collision be imminent limits the speed of assembling the truss in space. The approximate robot speed used in the tests reported herein will be required for assembly of the truss in space.

For a telerobotic in-space system to be feasible, the primary consideration is likely to be the ability of the operator to resolve all error conditions from the console without the need for extravehicular activity (EVA) support. Therefore, the error conditions and resolutions encountered during the test sequences were examined. Seventy errors occurred during the installation of 59 struts in one assembly test and 52 errors occurred during the assembly of 41 struts in the second assembly test. The operator required, on average, about 2 min to analyze the condition and correct the error with specially developed error menu routines. Most errors were associated with positioning the end effector at the truss and could not be corrected by passive guidance features incorporated into the current design of the end effector and joint receptacle. The operator was successful in correcting the positioning errors with the support of a limited video surveillance system; however, the reliance on taught points developed in a $1g$ test system appears inadequate for

space operations. Simulating $0g$ positioning, as well as all thermal conditions that are required for the accurate positioning of an end effector during space operation in a terrestrial laboratory, would be difficult. These difficulties highlight the need for a machine vision capability to discriminate a passive target and provide range and positioning information to guide a robot for close proximity positioning. Preliminary tests on a machine vision system have been conducted in a subsequent investigation and the results appear promising.

The tests conducted in the current investigation were successful in performing the autonomous telerobotic assembly of the complete truss. A significant portion of the system capability was empirically developed, and a number of conditions were encountered which would not have been readily anticipated or incurred through simulation studies. The tests were conducted in a $1g$ laboratory environment without gravity compensation; therefore, a larger number of installation conditions had to be accounted for than would be required for an automated system operating in space. Addressing the total integrated task, instead of bench testing of component parts, forced all aspects of the task to be evaluated. Although the current test results indicate that additional developments in specific areas need to be examined, automated assembly of truss structures in space for precision antennas is a desirable and viable construction method.

NASA Langley Research Center
Hampton, VA 23681-0001
April 22, 1994

Appendix

Assembly Rules

Key information for the strut assembly sequence developed for the tests reported in this paper are shown in table A1. The "Strut number" represents the order in which the struts were installed as shown in figure 16. The "Strut name" is the identifier defined in the "Truss" section and includes the ring number (R_), cell number (C_), and clock positions of the connecting nodes from the operators perspective and described in the section "Installation Positions and Robot-Arm Assembly Paths." The heading "Installation condition" defines the connectivity condition for this strut. The three potential conditions are direct, capture, and pyramid completion. Those struts labeled "direct" without a modifier ("top" or "bottom") are installed into receptacles fixed at both ends. The struts with a modifier are installed on one end only and left cantilevered with the preattached node in either the top or bottom face of the truss as indicated by the suffix modifier. The "Robot reference condition" indicates the actual ring and cell in figure 16 where the robot is located for installation and the strut path used by the robot for installation of the member. All paths are referenced to a member in either of the two cell types shown in figure 14. Most are referenced to ring 1 cell 1 (R1C1) of the test truss, which has the same orientation as cell A in figure 14. The remainder are referenced to paths in ring 2 cell 1 (R2C1), which is an inverted cell (designated by a prefix V) labeled as cell B in figure 14. The heading "Motion-base position" defines the displacement of the base of the robot with respect to the reference cell for which the installation path was taught and the angle of the rotational motion base. The headings "Pallet," "Slot," and "Node end" define the pallet and slot where each strut is located and the end of the strut that contains a preattached node. The node locations in the pallet are identified as "R" for right and "L" for left from the view point of an observer looking in the U-direction of the robot coordinate system (fig. 2(b)). When all pallets are filled in the supply canister, the pallet at the top is designated as the number 1 pallet, and the slot nearest the robot is the number 1 slot.

The assembly sequence illustrated was developed manually by using a set of guidelines that related the general operational characteristics of the system, structural considerations of the assembled components, and packaging constraints. Most of the rules would apply for assembly in space of structures of this type; however, some rules were dictated by the $1g$ environment. As indicated by examining figure 16, assembly starts by installing the six struts that form the center tetrahedron. Because a tetrahedron is a stable truss unit, much of the assembly sequence is developed around building tetrahedrons and connecting them. The tetrahedrons are connected to form rings and the first ring, consisting of 24 struts, is completed before installing any members in the second ring. The second ring is assembled in two parts. The lower section which has nodes only in the bottom face is assembled first. Then, the upper section, which has nodes only in the top face, is assembled. This procedure was used as a convenience in tracking struts so as not to inadvertently miss or block a strut during the development. Also, minimizing the number of motion-base moves so that as many struts as possible were installed with the motion bases at a given position was desirable. Also, minimizing the number of different axes involved in motion-base moves was considered. The number of taught installation points and associated robot paths were minimized, although as indicated, the total assembly required 19 different installation paths to be defined.

Two factors had a significant impact on the development of the assembly plan. First, early in the program all operations were attempted in the $1g$ laboratory environment without special supports or gravity compensation devices. Therefore, only core struts were installed at one end and left in a cantilevered condition to minimize the gravity deformation. After each core strut was installed, a face strut was installed between the free end of the cantilevered strut and a fixed node. A strut was never cantilevered from the free end of another cantilevered strut. Second, the core members with preattached nodes had to be available and accessible in the pallet. A limited number of struts with nodes could be stored in each pallet and there was no provision for detaching a node and moving it from one strut to another. Also, no consideration was given to removing struts from pallets that were located in the storage canister. All struts had to be removed from a pallet before it was transferred; therefore, some slots in selected pallets had to be left vacant. Also, because of compact packaging, the struts in the pallet with nodes had to be removed before the adjacent struts without nodes could be accessed because the end effector would collide with the receptacles on the adjacent node. Coordination between the structural aspects of the assembly operation, and the availability and accessibility of struts in the pallets, limits the number of options in selecting struts for installation.

Table A1. Strut Assembly Sequence

Strut number	Strut name (a)	Installation condition	Robot reference condition (a)	Motion-base position			Pallet	Slot	Node end (b)
				X, m	Y, m	Θ, deg			
Center pyramid									
1	R1C1/10_2	Direct	R1C1/10_2	0	0	0	1	3	
2	R1C1/12_2	Direct/top	R1C1/12_2			0		5	L
3	R1C3/6_10	Direct	R1C1/10_2			120		4	
4	R1C3/8_10	Capture	R1C1/12_2			120		6	
5	R1C2/6_2	Direct	R1C1/10_2			−120		7	
6	R1C2/6_4	Pyd. comp.	R1C1/12_2			−120		11	
First ring									
7	R1C2/12_2	Direct/top	R1C1/F10_8	0	0	−120	1	9	L
8	R1C2/12_4	Capture	R1C1/12_8		0			8	
9	R2C7/6_4	Direct/top	R1C1/12_2		2			13	L
10	R2C7/8_4	Capture	R1C1/12_4		2			10	
11	R1C3/12_8	Pyd. comp.	R1C1/12_4		0	120		12	
12	R1C3/6_4	Direct/top	R1C1/F10_8		0			1	L
13	R1C3/8_4	Capture	R1C1/12_8		0			2	
14	R2C1/10_8	Direct/top	R1C1/F12_2		2		2	5	R
15	R2C1/12_8	Capture	R1C1/12_4		2			4	
16	R1C1/12_4	Pyd. comp.	R1C1/12_4		0	0		6	
17	R1C1/10_8	Direct/top	R1C1/10_8		0			9	R
18	R1C1/12_8	Capture	R1C1/12_8		0			7	
19	R2C4/12_2	Direct/top	R1C1/F12_2		2			13	R
20	R2C4/12_4	Capture	R1C1/12_4		2			8	
21	R1C2/8_4	Pyd. comp.	R1C1/12_4		0	−120		11	
22	R1C2/12_8	Direct	R1C1/8_4			−120		12	
23	R1C3/12_4	Direct	R1C1/8_4			120		3	
24	R1C1/8_4	Direct	R1C1/8_4			0		10	
Second ring (lower section)									
25	R1C2/10_8	Direct/btm	R1C1/F6_4	0	0	−120	2	1	R
26	R1C2/6_10	Capture	R1C1/6_2	0	0		2	2	
27	R1C2/10_2	Pyd. comp.	R1C1/6_10	0	0		3	1	
28	R2C6/6_4	Direct	R1C1/12_2	1.73	1			5	
29	R2C7/10_8	Direct/btm	R1C1/6_4	0	2			3	L
30	R2C7/6_10	Capture	R1C1/6_2	0	2			2	
31	R2C6/6_2	Pyd. comp.	R1C1/10_2	1.73	1			4	
32	R2C8/10_8	Direct/btm	R1C1/F12_2	1.73	−1	120		7	L

[a]Strut name and robot reference condition:
R Truss ring C Truss cell
F Flipped path V Inverted cell

[b]Node end:
R Right end of pallet
L Left end of pallet

Table A1. Continued

Strut number	Strut name (a)	Installation condition	Robot reference condition (a)	Motion-base position			Pallet	Slot	Node end (b)
				X, m	Y, m	Θ, deg			
33	R2C7/6_2	Capture	R2C1/V6_2	0	0	−180	3	6	
34	R2C7/10_2	Pyd. comp.	R2C1/V10_2			−180		8	
35	R1C3/12_2	Direct/btm	R1C1/6_4			120		11	L
36	R1C3/10_2	Capture	R1C1/6_2					9	
37	R1C3/6_2	Pyd. comp.	R1C1/6_10					10	
38	R2C9/10_8	Direct	R1C1/12_2	1.73	1			12	
39	R2C1/12_2	Direct/btm	R1C1/F6_4	0	0		4	3	R
40	R2C1/10_2	Capture	R1C1/6_2	0	2			1	
41	R2C9/6_10	Pyd. comp.	R1C1/10_2	1.73	1			2	
42	R2C2/12_2	Direct/btm	R1C1/12_2	1.73	−1	0		7	R
43	R2C1/6_10	Capture	R2C1/V6_2	0	0	60		4	
44	R2C1/6_2	Pyd. comp.	R2C1/V10_2			60		5	
45	R1C1/6_4	Direct/btm	R1C1/F6_4			0		11	R
46	R1C1/6_2	Capture	R1C1/6_2					6	
47	R1C1/6_10	Pyd. comp.	R1C1/6_10					8	
48	R2C3/12_2	Direct	R1C1/12_2	1.73	1			9	
49	R2C4/6_4	Direct/btm	R1C1/6_4	0	2		5	5	L
50	R2C4/2_6	Capture	R1C1/6_2	0	2			4	
51	R2C3/10_2	Pyd. comp.	R1C1/10_2	1.73	1			3	
52	R2C5/6_4	Direct/btm	R1C1/12_2	1.73	−1	−120		9	L
53	R2C4/10_2	Capture	R2C1/V6_2	0	0	−60		8	
54	R2C4/10_6	Pyd. comp.	R2C1/V10_2	0	0	−60		7	
55	R2C5/2_6	Direct	R1C1/10_2	1.73	−1	−120		6	
56	R2C8/10_6	Direct	R1C1/10_2	1.73	−1	120		10	
57	R2C2/10_2	Direct	R1C1/10_2	1.73	−1	0		11	
Lower ring (top section)									
58	R3C7/4_2	Direct/top	R2C1/V12_2	0	0	−30	5	13	L
59	R2C4/12_8	Capture	R2C1/V12_4	0	0	−30		12	
60	R3C7/12_2	Direct/top	R1C1/F10_8	1.73	−3	−120		1	L
61	R3C7/12_4	Capture	R2C1/V8_4	1.73	1	−60		2	
62	R2C5/8_4	Pyd. comp.	R1C1/12_4	1.73	−1	−120	6	3	
63	R3C12/6_8	Direct/top	R2C1/FV12_2	0	0	−150		1	R
64	R2C7/12_4	Capture	R2C1/V12_4	0	0	150		2	
65	R3C12/6_4	Direct/top	R1C1/10_8	1.73	−3	120		5	R
66	R3C12/8_4	Capture	R2C1/V8_4	1.73	1	180		4	
67	R2C8/12_8	Pyd. comp.	R1C1/12_4	1.73	−1	120		6	
68	R2C7/12_8	Direct	R1C1/8_4	0	2	−120		7	
69	R3C11/6_4	Direct	R2C1/V12_10	0	0	180		11	

[a]Strut name and robot reference condition:
R Truss ring C Truss cell
F Flipped path V Inverted cell

[b]Node end:
R Right end of pallet
L Left end of pallet

Table A1. Concluded

Strut number	Strut name (a)	Installation condition	Robot reference condition (a)	Motion-base position			Pallet	Slot	Node end (b)
				X, m	Y, m	Θ, deg			
70	R2C6/12_2	Direct/top	R1C1/10_8	1.73	1	−120	6	9	R
71	R2C6/12_4	Capture	R1C1/12_8	↓	1	−120	↓	8	
72	R3C11/8_4	Pyd. comp.	R2C1/V8_4		−1	180		10	
73	R2C5/12_2	Direct/top	R1C1/10_8		−1	−120		13	R
74	R2C5/12_4	Capture	R1C1/12_8		−1	↓		12	
75	R2C6/8_4	Pyd. comp.	R1C1/12_4		1		7	1	
76	R2C6/12_8	Direct	R1C1/8_4		1		↓	5	
77	R2C5/12_8	Direct	R1C1/8_4	↓	−1	↓		9	
78	R3C2/12_10	Direct/top	R2C1/V12_2	0	0	90		7	L
79	R2C1/8_4	Capture	R2C1/V12_4	0	0	90		8	
80	R3C2/10_8	Direct/top	R1C1/F10_8	1.73	−3	0		11	L
81	R3C1/12_8	Capture	R2C1/V8_4	1.73	1	60		12	
82	R2C2/12_4	Pyd. comp.	R1C1/12_4	1.73	−1	0		13	
83	R2C4/8_4	Direct	R1C1/8_4	0	2	0		10	
84	R3C6/12_2	Direct	R2C1/V12_10	0	0	−60		6	
85	R2C3/10_8	Direct/top	R1C1/F10_8	1.73	1	0		3	L
86	R2C3/12_8	Capture	R1C1/12_8	↓	1	0		2	
87	R3C6/12_4	Pyd. comp.	R2C1/V8_4		−1	−60	↓	4	
88	R2C2/10_8	Direct/top	R1C1/10_8		−1	0	8	3	R
89	R2C2/12_8	Capture	R1C1/12_8		−1	↓	↓	2	
90	R2C3/12_4	Pyd. comp.	R1C1/12_4		1			1	
91	R2C3/8_4	Direct	R1C1/8_4		1			4	
92	R2C2/8_4	Direct	R1C1/8_4	↓	−1	↓		5	
93	R2C1/12_4	Direct	R1C1/8_4	0	2	120		9	
94	R3C1/10_8	Direct	R2C1/V12_10	0	0	60		13	
95	R2C9/6_4	Direct/top	R1C1/10_8	1.73	1	120		11	R
96	R2C9/8_4	Capture	R1C1/12_8	↓	1	120		10	
97	R3C1/12_8	Pyd. comp.	R2C1/V8_4		−1	60		12	
98	R2C8/6_4	Direct/top	R1C1/10_8		−1	120		7	R
99	R2C8/8_4	Capture	R1C1/12_8		−1	↓		6	
100	R2C9/12_8	Pyd. comp.	R1C1/12_4		1		↓	8	
101	R2C9/12_4	Direct	R1C1/8_4		1		9	3	
102	R2C8/12_4	Direct	R1C1/8_4	↓	−1	↓	9	7	

[a]Strut name and robot reference condition:
R Truss ring C Truss cell
F Flipped path V Inverted cell

[b]Node end:
R Right end of pallet
L Left end of pallet

References

1. Swanson, Paul N.: *A Lightweight Low Cost Large Deployable Reflector (LDR) – A Concept Study by the Jet Propulsion Laboratory.* JPL D-2283, California Inst. of Technology, June 1985. U. S. Government Agencies only.

2. Wu, K. Chauncey; Adams, Richard R.; and Rhodes, Marvin D.: *Analytical and Photogrammetric Characterization of a Planar Tetrahedral Truss.* NASA TM-4231, 1990.

3. Rhodes, Marvin D.; Will, Ralph W.; and Wise, Marion A.: A Telerobotic System for Automated Assembly of Large Space Structures. *The 21st Century in Space, Volume 70 – Advances in the Astronautical Sciences*, George V. Butler, ed., American Astronaut. Soc., 1988, pp. 111–129. (Available as AAS 88-170.)

4. Monroe, Charles A., Jr.: Development of Cable Drive Systems for an Automated Assembly Project. *24th Aerospace Mechanisms Symposium*, NASA CP-3062, 1990, pp. 353–367.

5. Herstrom, Catherine L.; Grantham, Carolyn; Allen, Cheryl L.; Doggett, William R.; and Will, Ralph W.: *Software Design for Automated Assembly of Truss Structures.* NASA TP-3198, 1992.

6. Heard, Walter L., Jr.; Lake, Mark S.; Bush, Harold G.; Jensen, J. Kermit; Phelps, James E.; and Wallsom, Richard E.: *Extravehicular Activity Compatibility Evaluation of Developmental Hardware for Assembly and Repair of Precision Reflectors.* NASA TP-3246, 1992.

7. Sydow, P. Daniel; and Cooper, Eric G.: *Development of a Machine Vision System for Automated Structural Assembly.* NASA TM-4366, 1992.

8. Greene, William H.: Effects of Random Member Length Errors on the Accuracy and Internal Loads of Truss Antennas. *J. Spacecr. & Rockets*, vol. 22, no. 5, Sept.–Oct. 1985, pp. 554–559.

L-90-15358

Figure 1. Proposed submillimeter astronomical space telescope that incorporates a large precision truss-supported reflector.

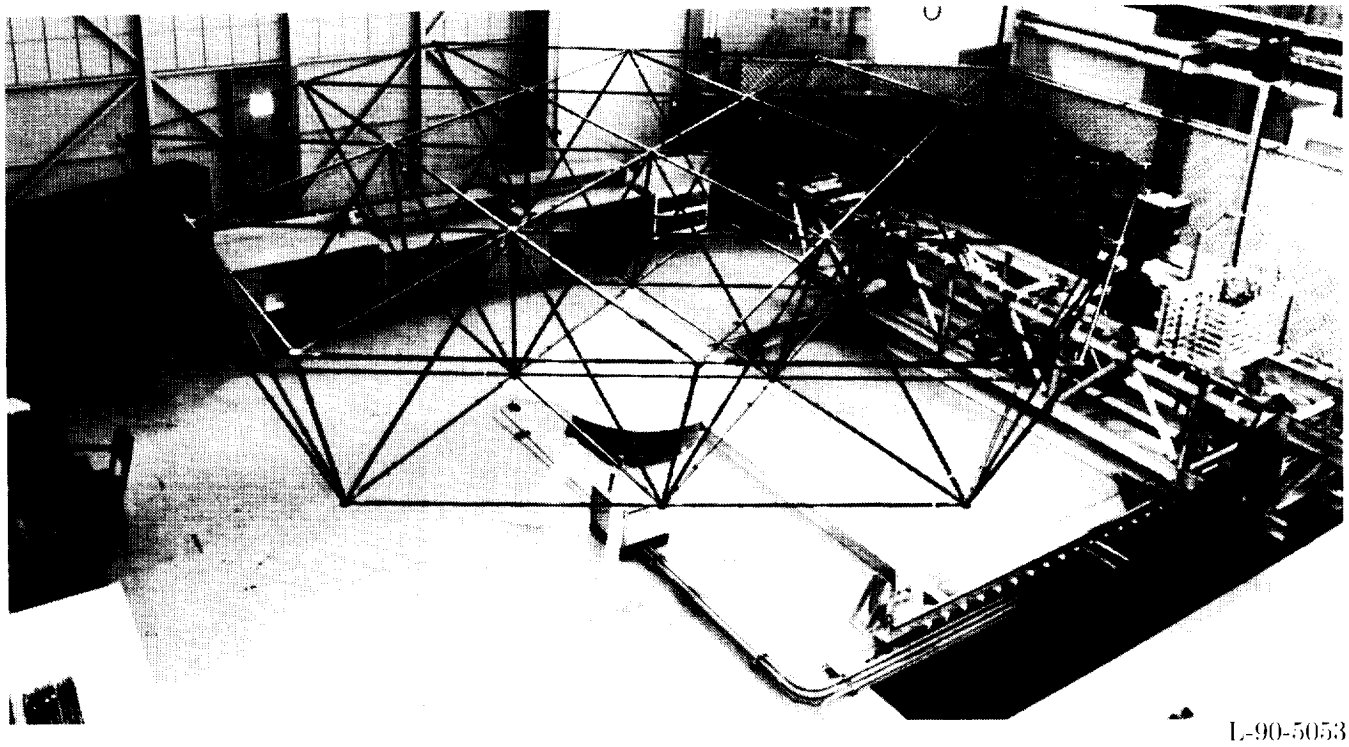

(a) Truss assembly hardware.

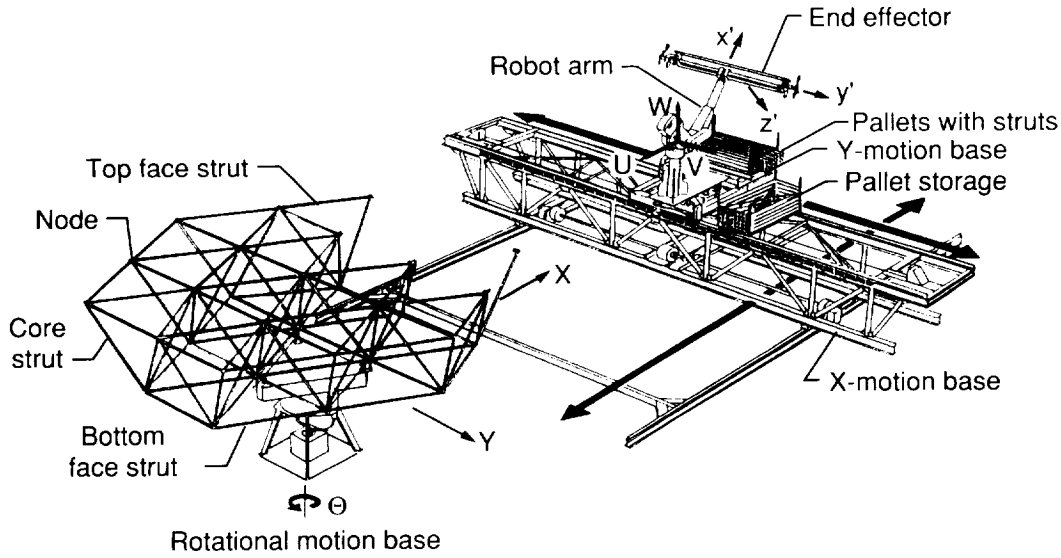

(b) Schematic of facility components and coordinate reference frames.

Figure 2. Test laboratory developed to perform operational studies of automated assembly of truss structures.

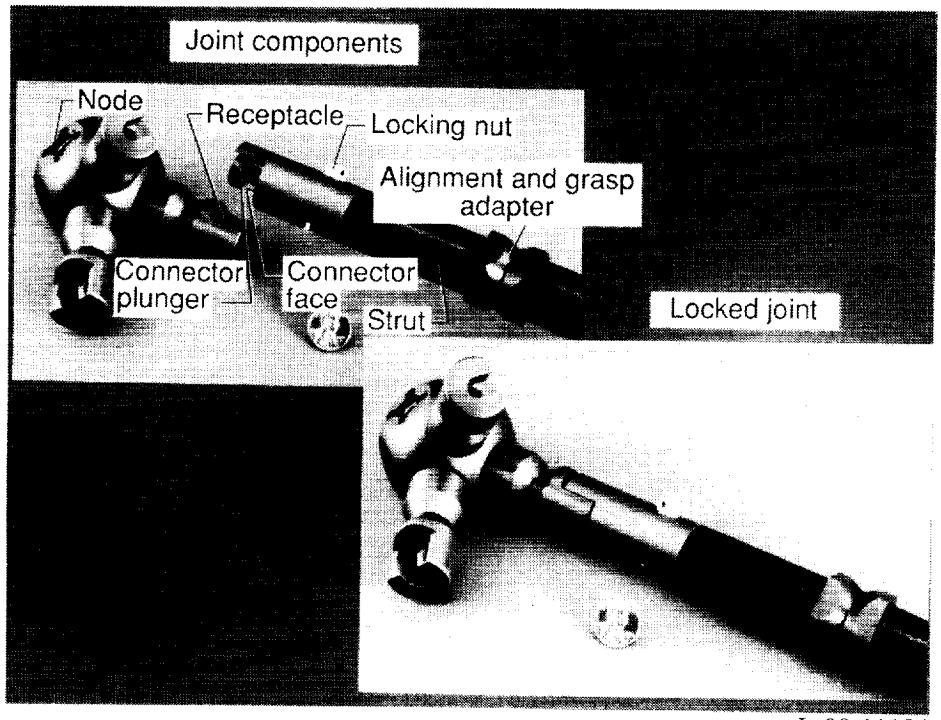

L-90-11104

Figure 3. Typical truss joint and node.

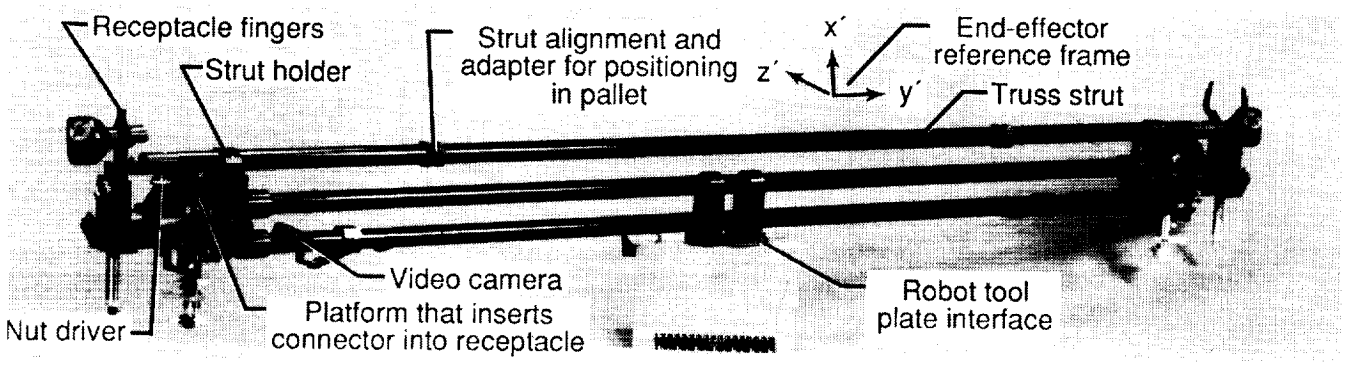

L-88-10,918

Figure 4. Truss assembly end effector.

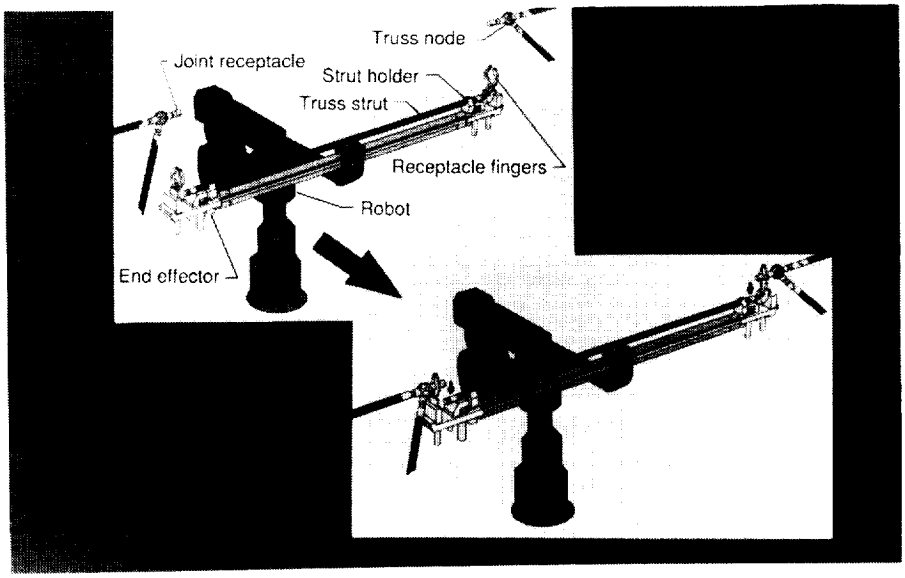

Figure 5. Artist sketch of robot with the end effector.

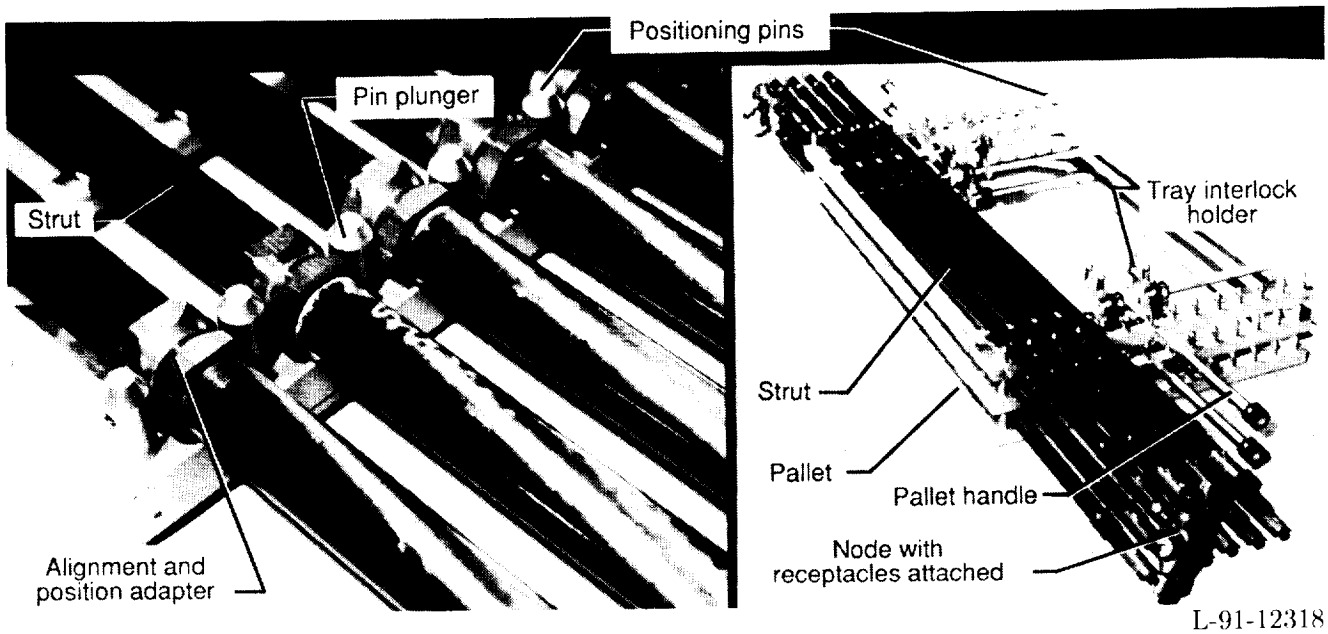

Figure 6. Struts in storage pallets.

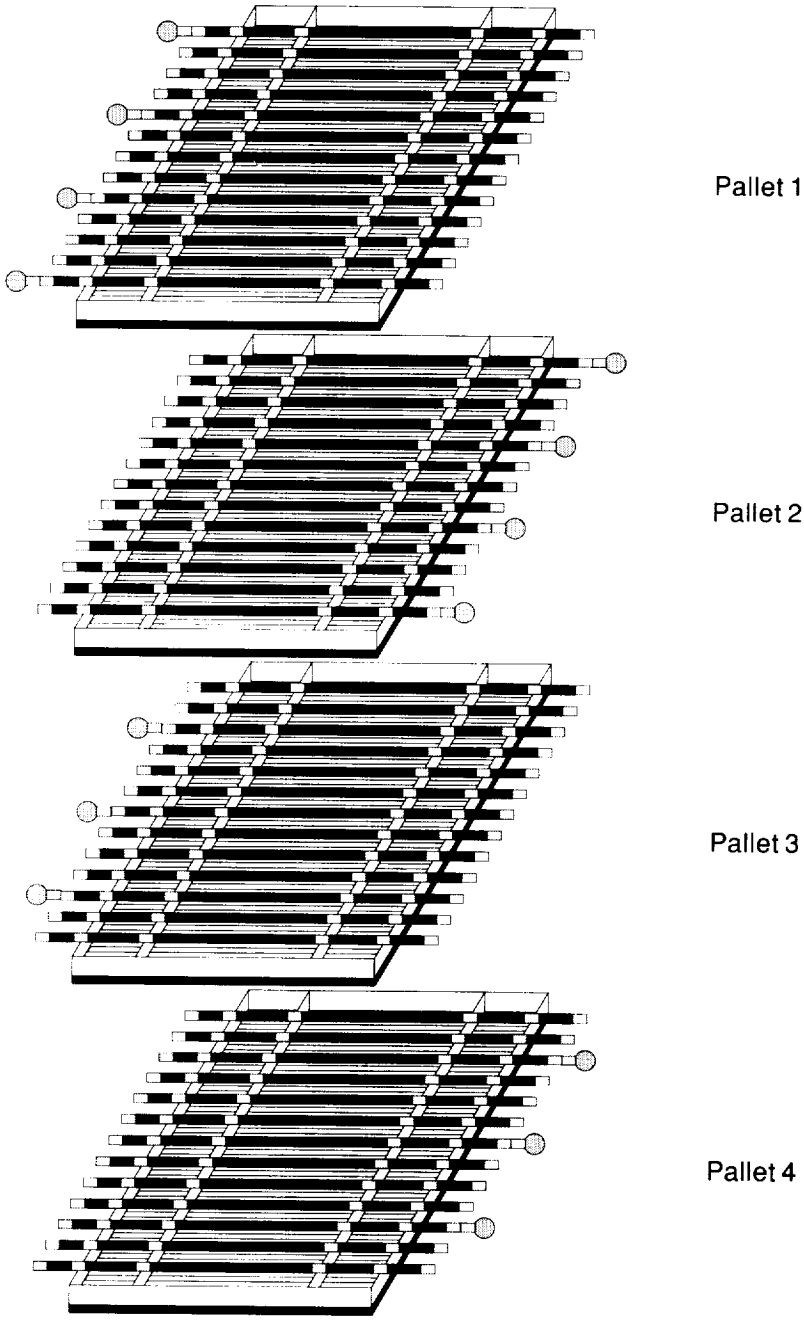

Figure 7. Arrangement of struts in pallets and stacking pattern of four pallet set.

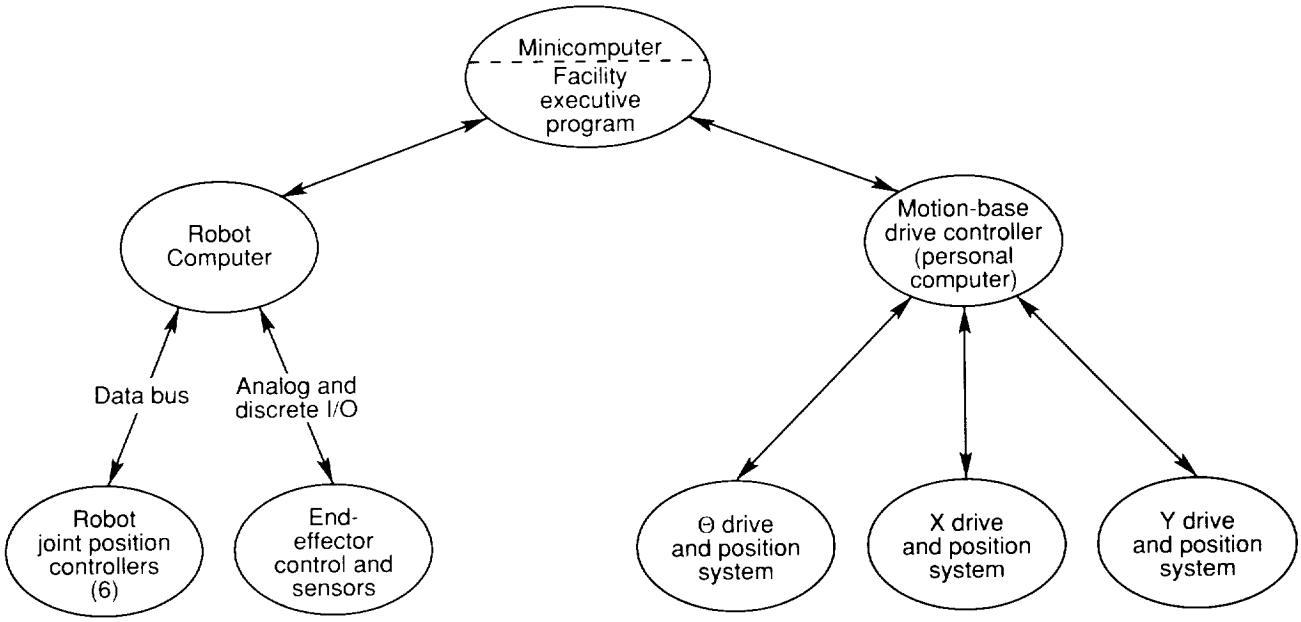

Figure 8. Schematic of computer control system.

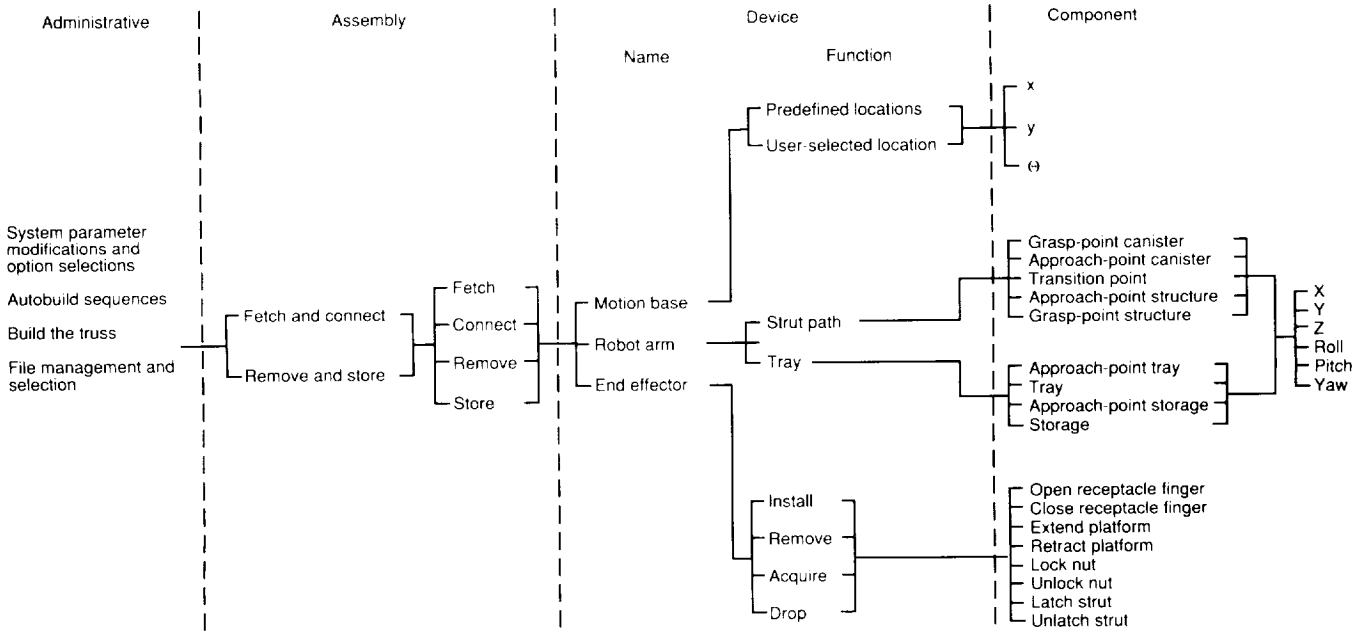

Figure 9. Design layout of executive software program.

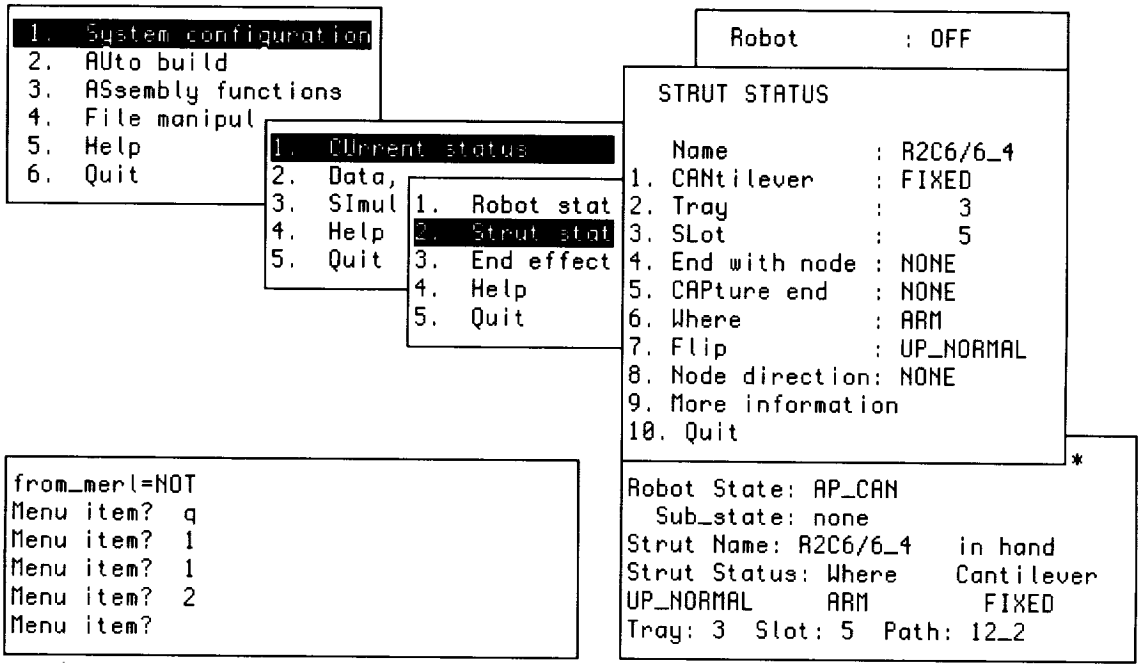

(a) Typical menus available to operator.

Figure 10. Basic menu layout of automated assembly system software.

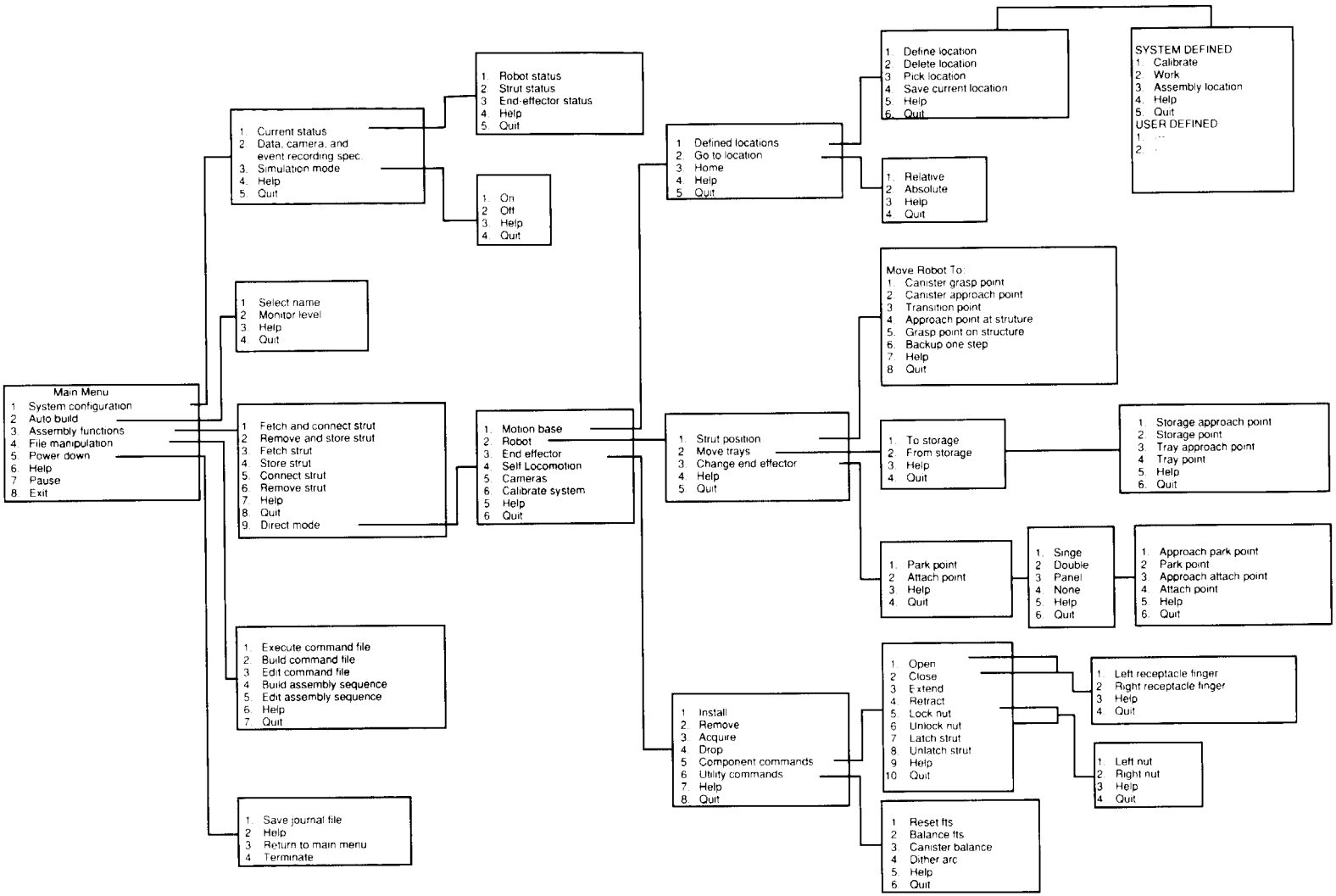

(b) Operator menus and their connectional relation.

Figure 10. Concluded.

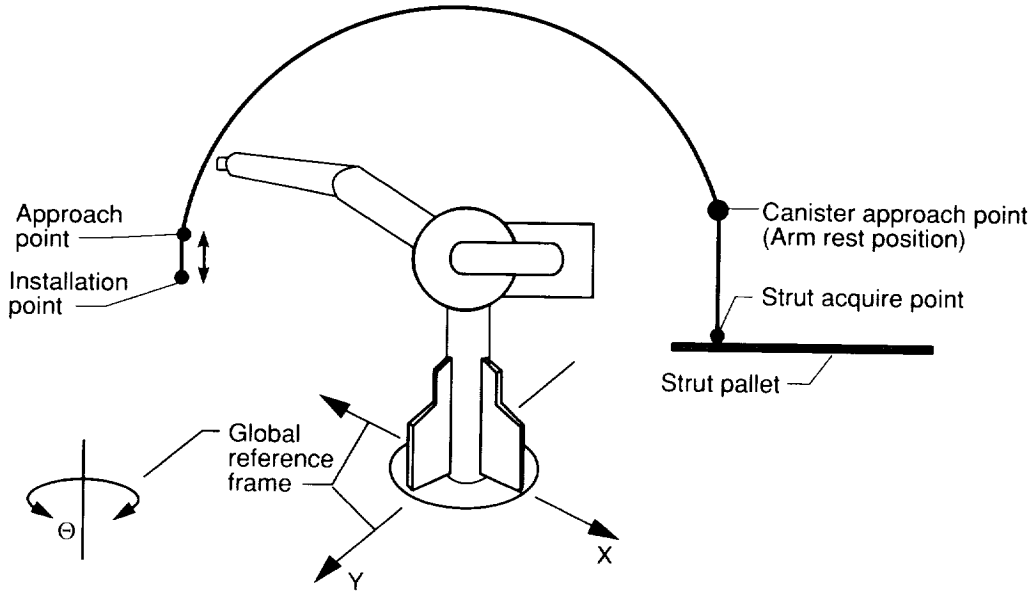

Figure 11. Path of robot arm for strut acquisition and installation.

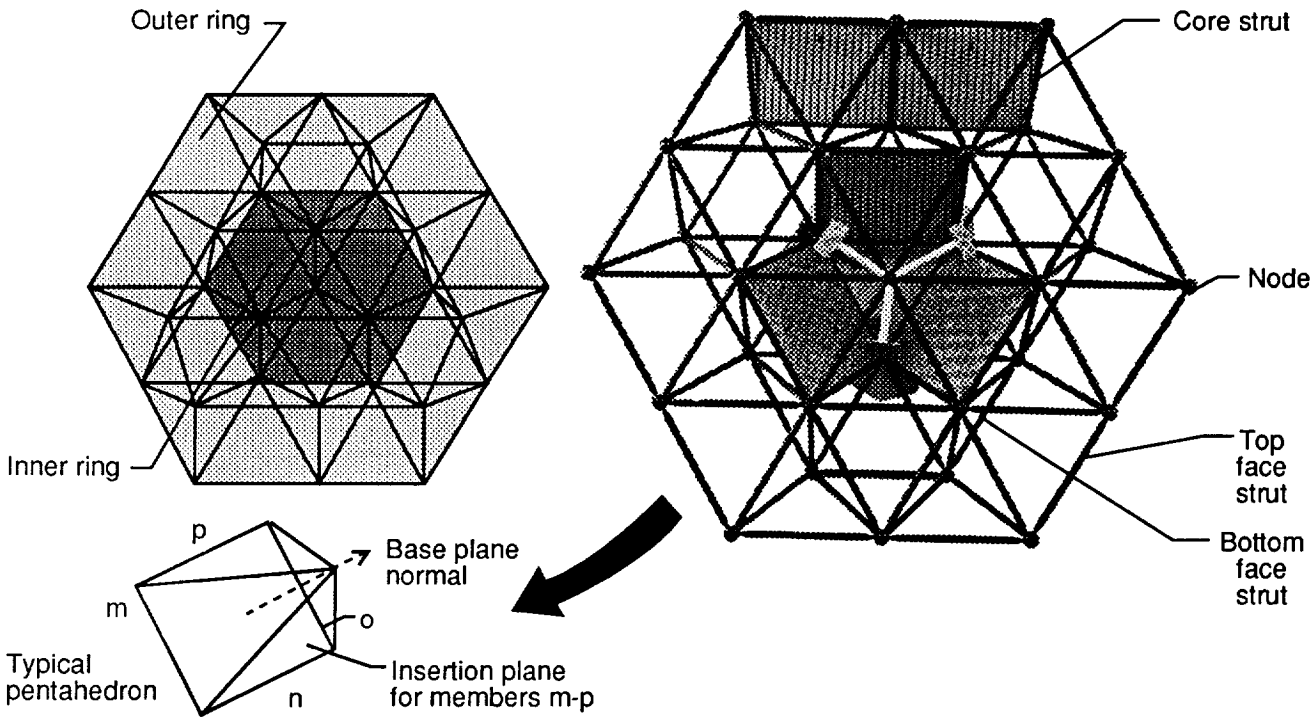

Figure 12. Tetrahedral truss used in assembly tests.

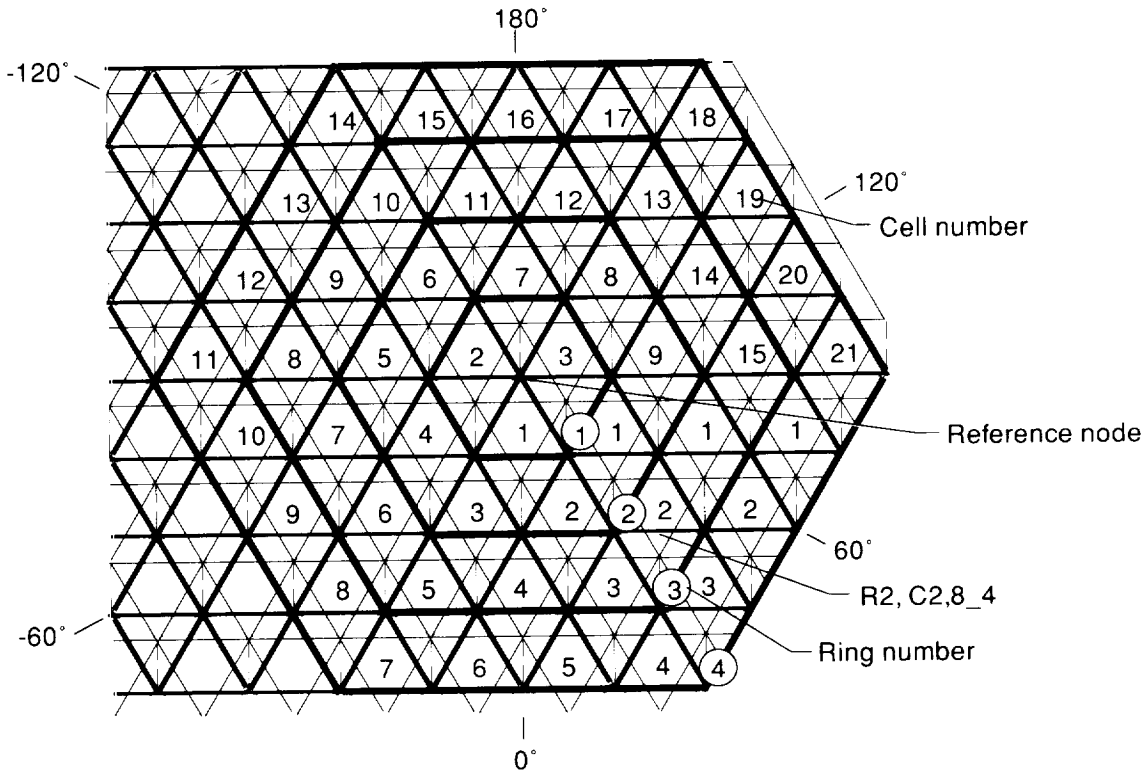

(a) Concentric hexagonal rings of large planar truss.

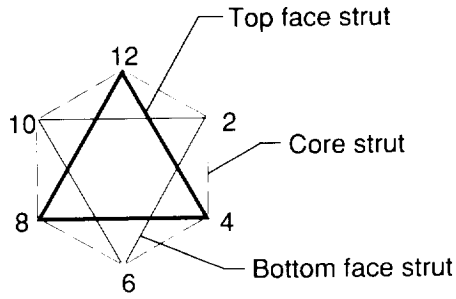

(b) Typical cell.

Figure 13. Planform sketch of large planar tetrahedral truss with naming convention identifiers.

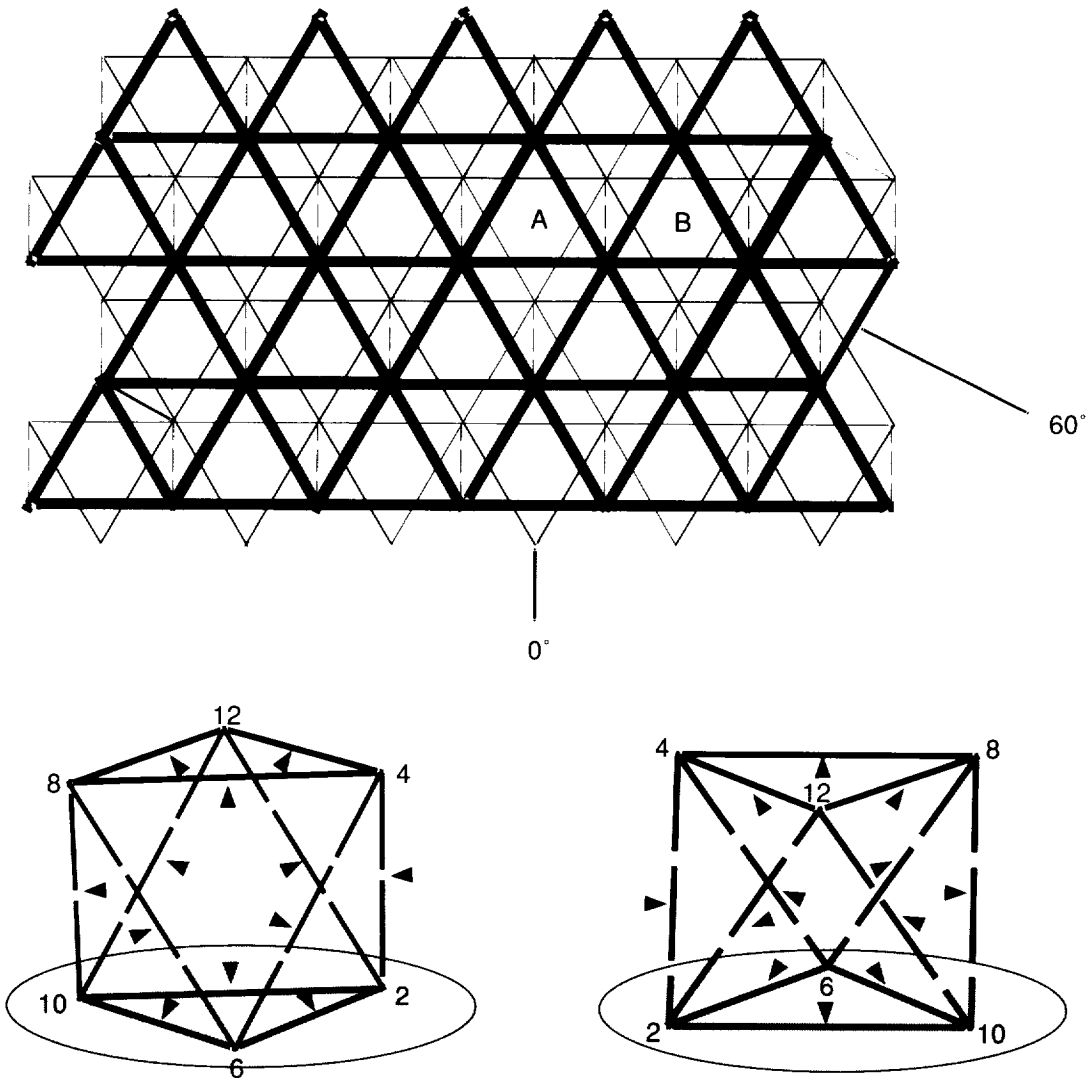

Axonometric view of cell A.

Axonometric view of cell B turned 60°.

Figure 14. Positions for installing struts in the truss.

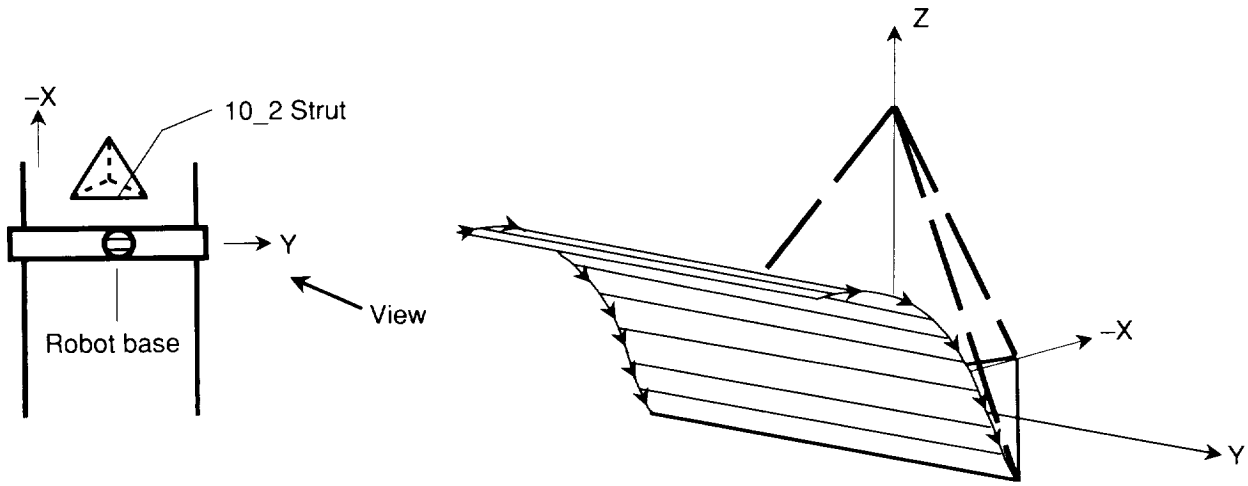

(a) Path and position for typical 10_2 strut.

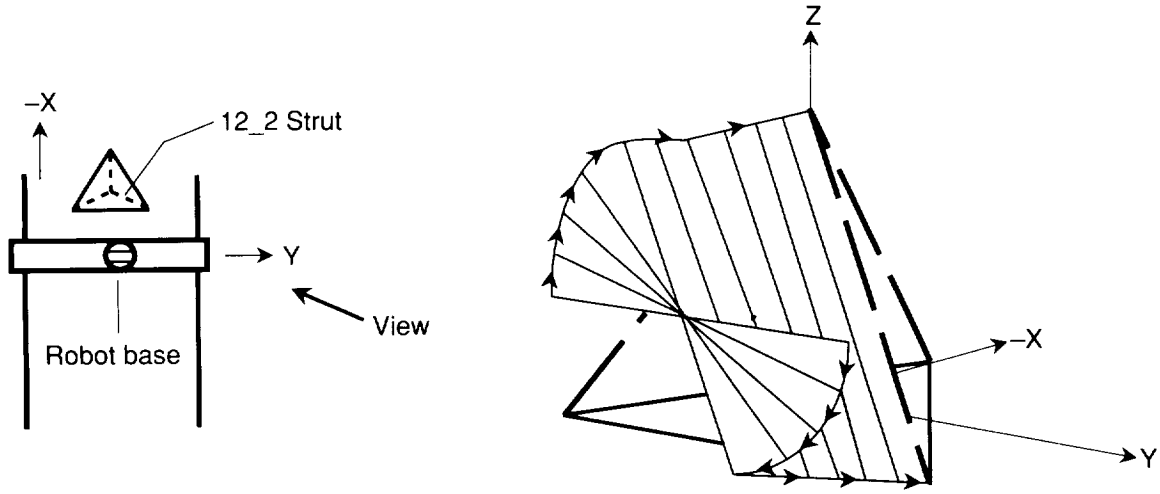

(b) Path and position for typical 12_2 strut.

Figure 15. Typical strut installation paths and positions.

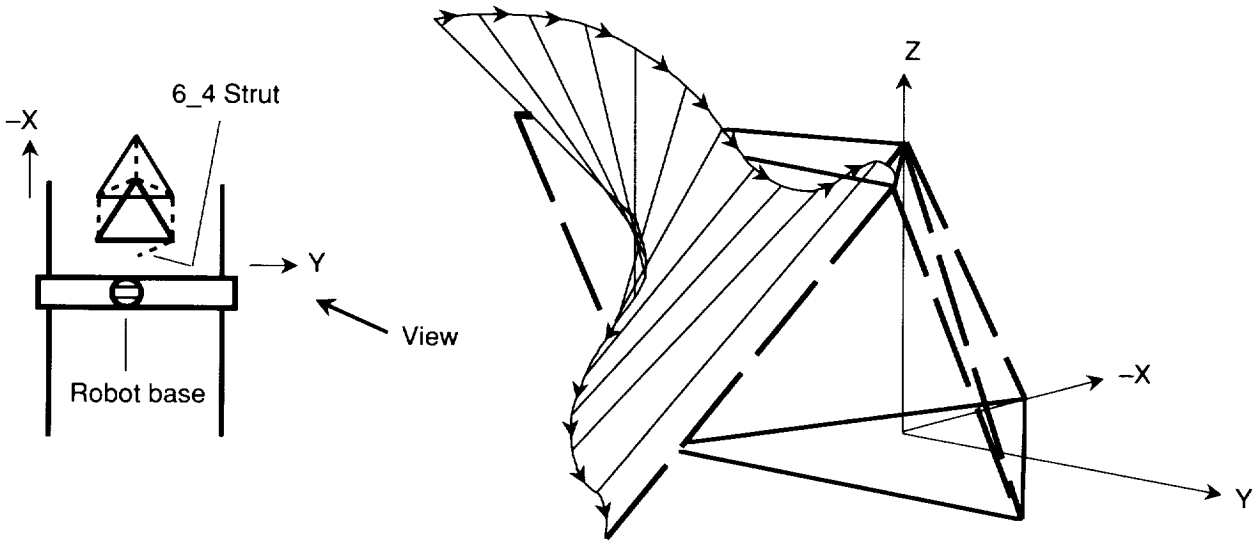

(c) Path and position for typical 6_4 strut.

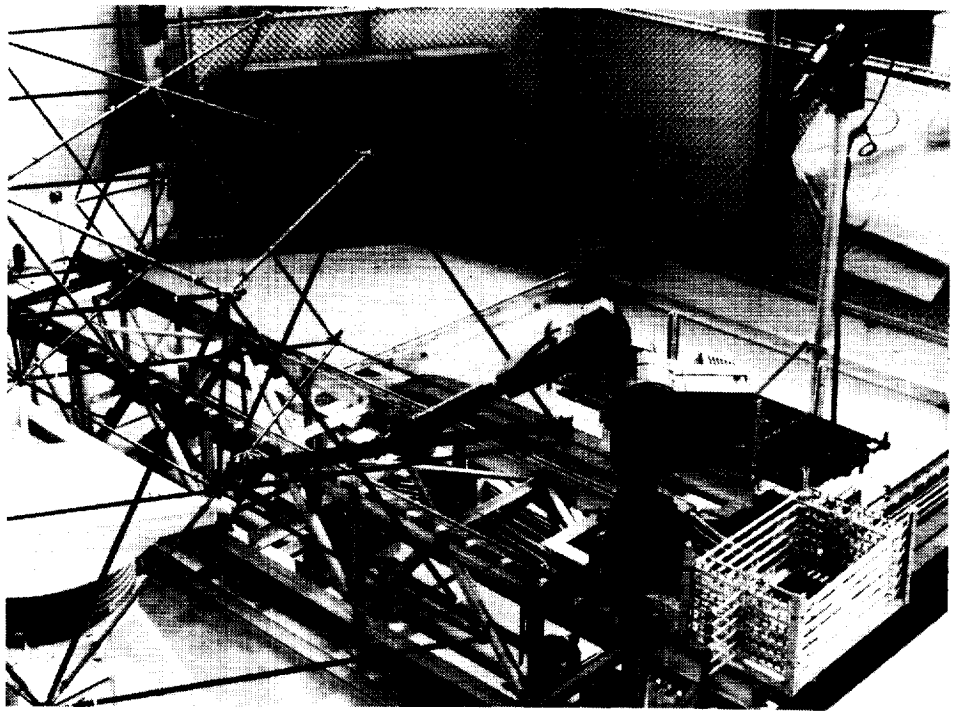

L-90-09365

(d) End effector at the approach point for a typical 6_2 strut.

Figure 15. Concluded.

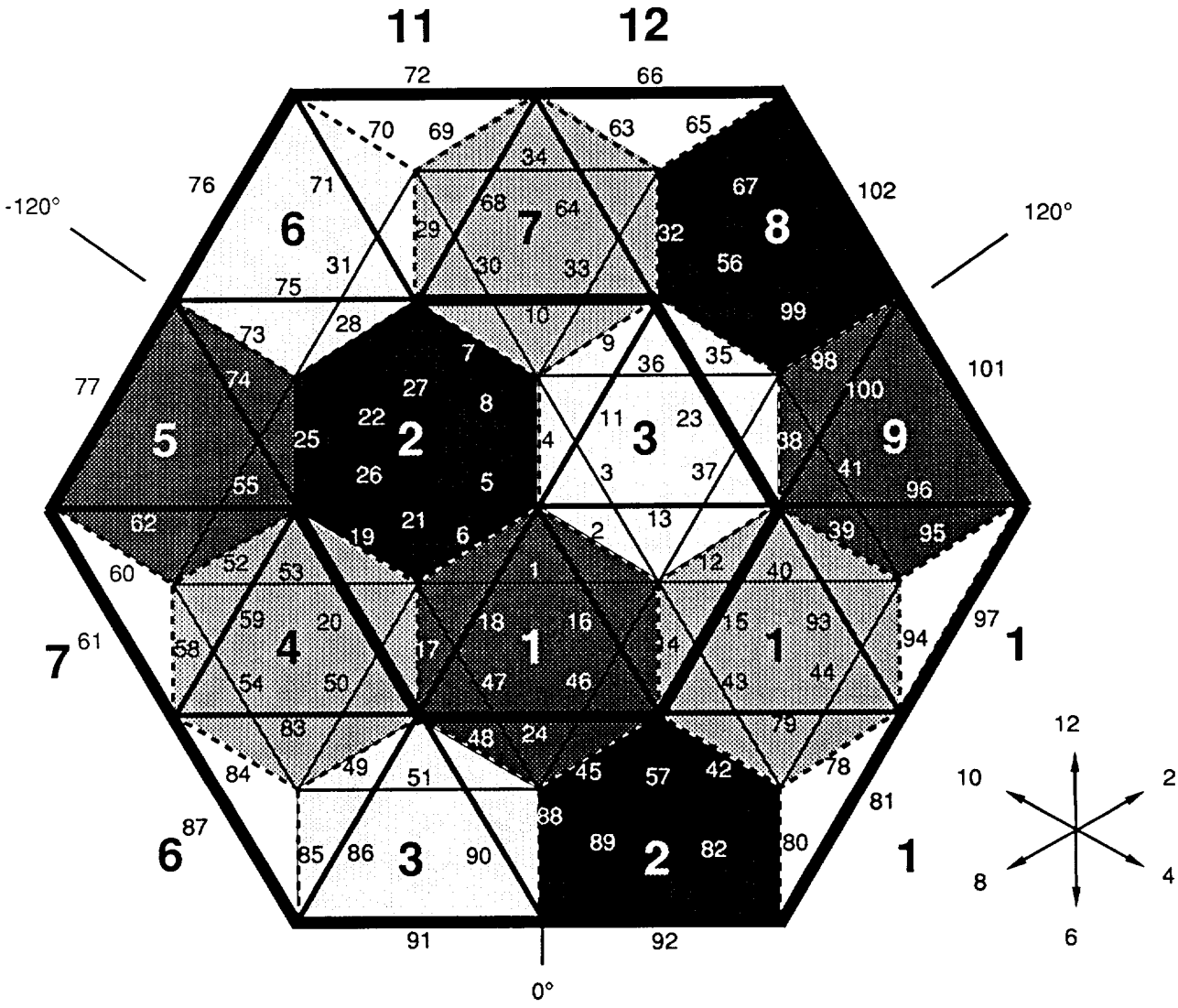

Figure 16. Sketch identifying truss cells and strut assembly sequence.

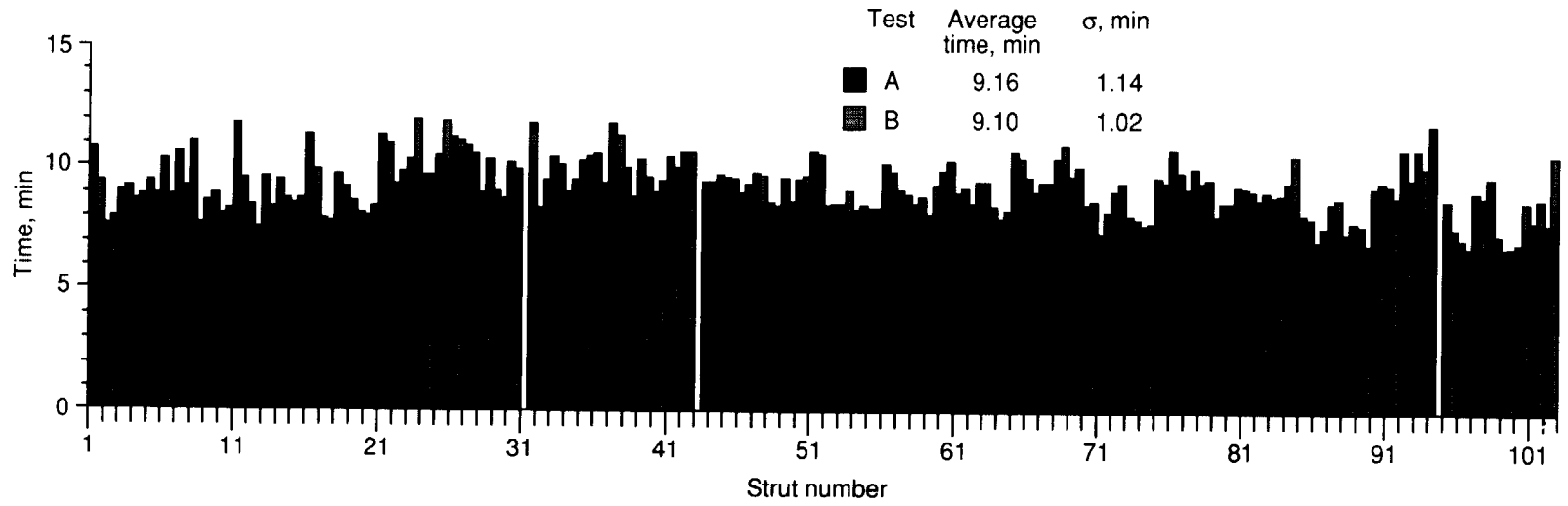

(a) Assembly tests.

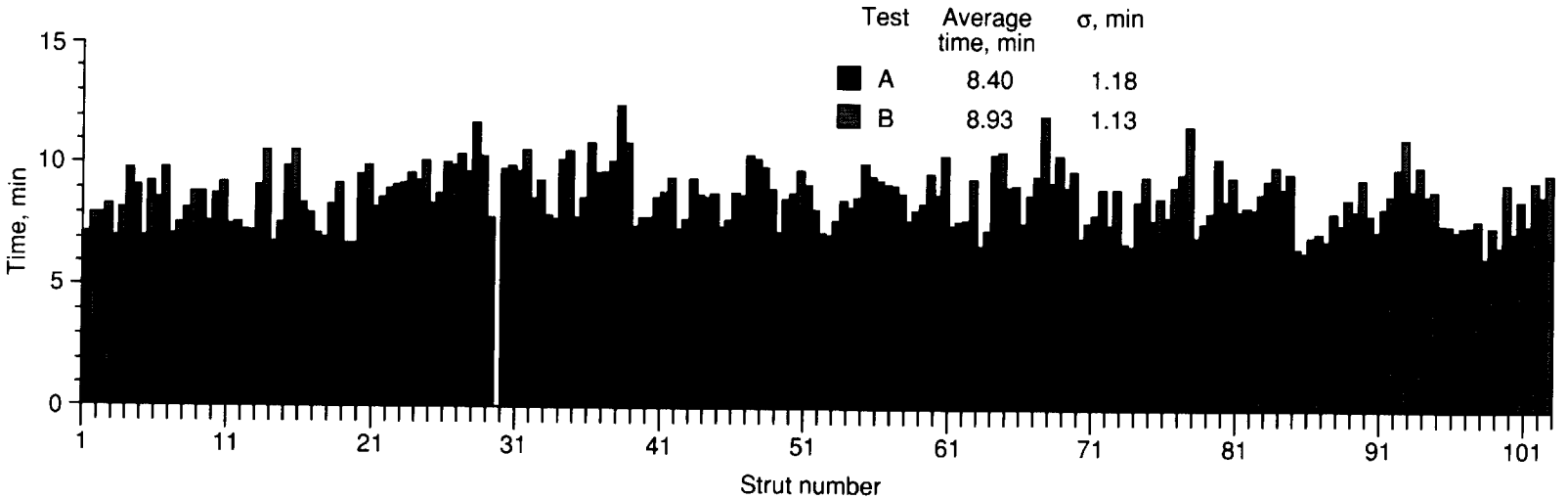

(b) Disassembly tests.

Figure 17. Total time required to acquire and install each strut during assembly and to remove and store each strut during disassembly for two tests.

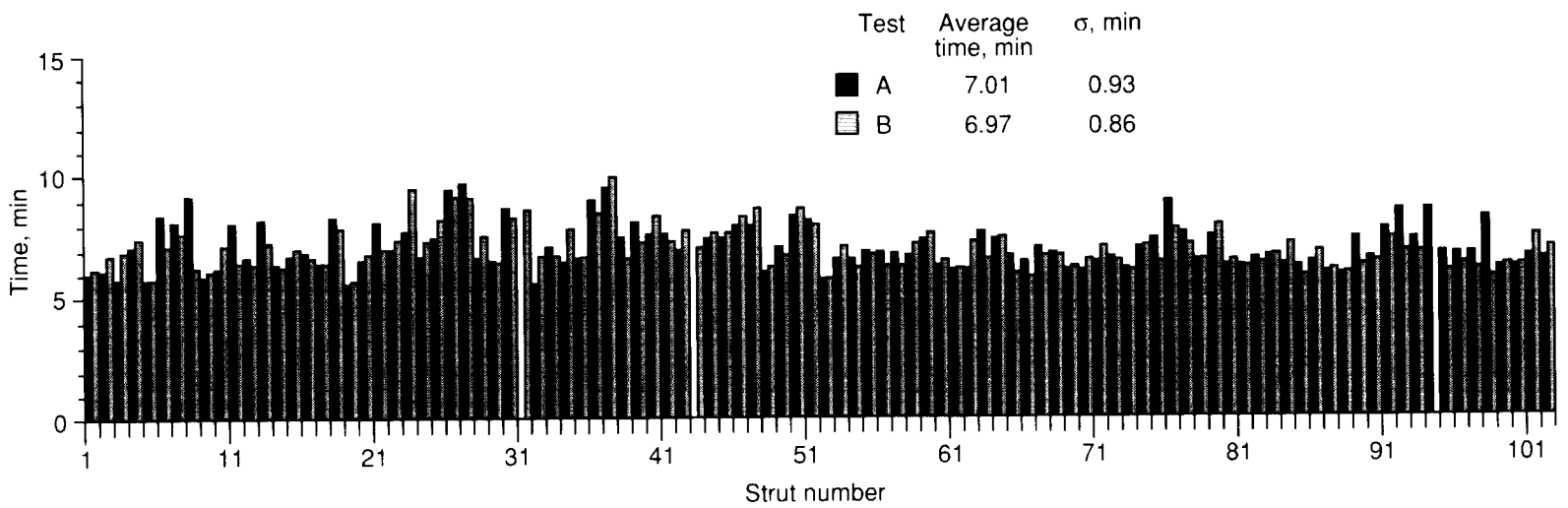

(a) Assembly tests.

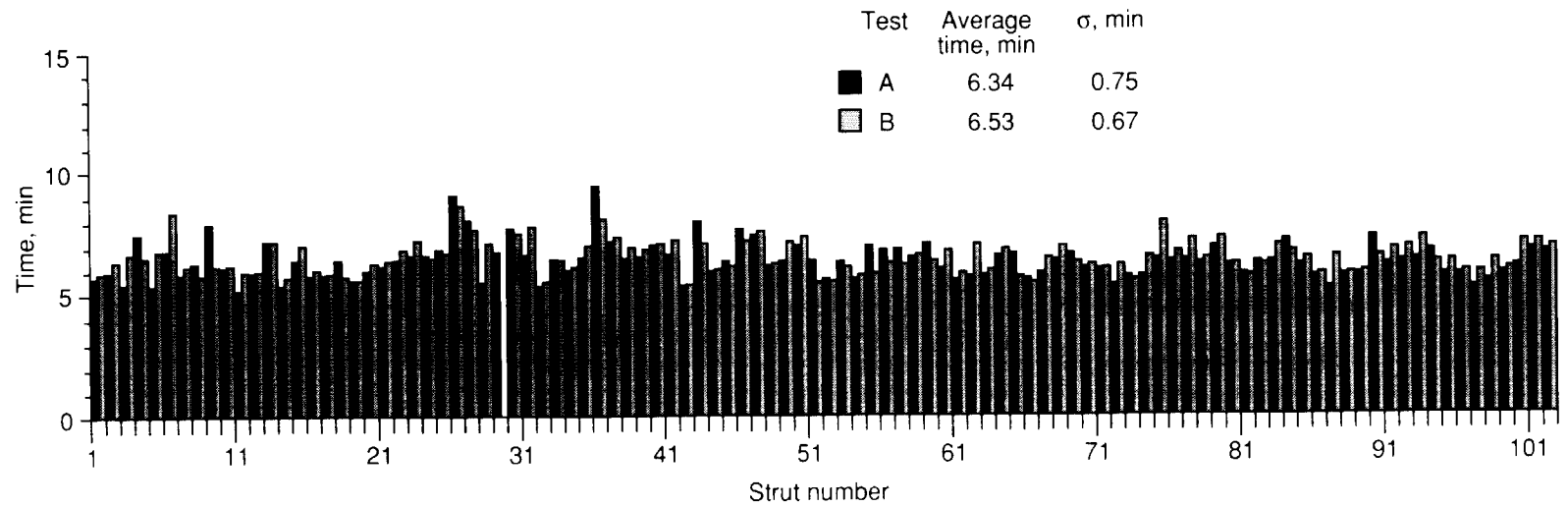

(b) Disassembly tests.

Figure 18. The time required to acquire and install each strut and to remove and store each strut without force-torque repositioning and motion base positioning.

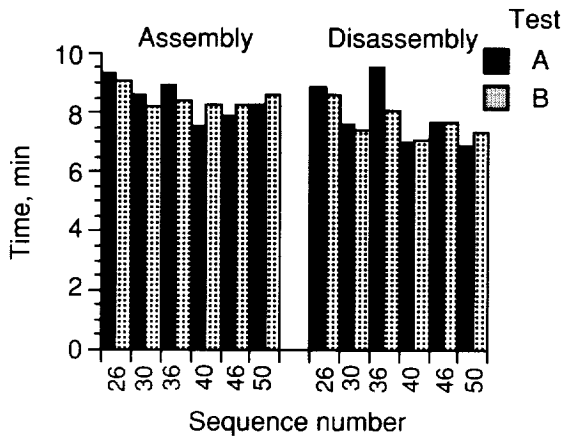

(a) 6_2 Path; capture installation.

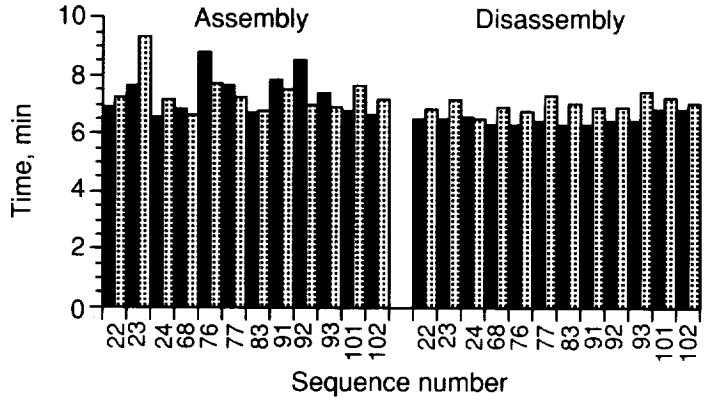

(b) 8_4 Path; direct installation.

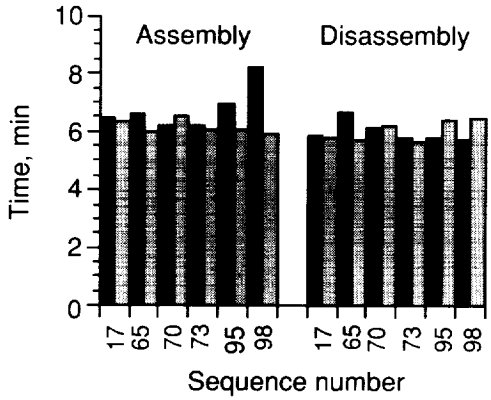

(c) 10_8 Path; cantilever installation.

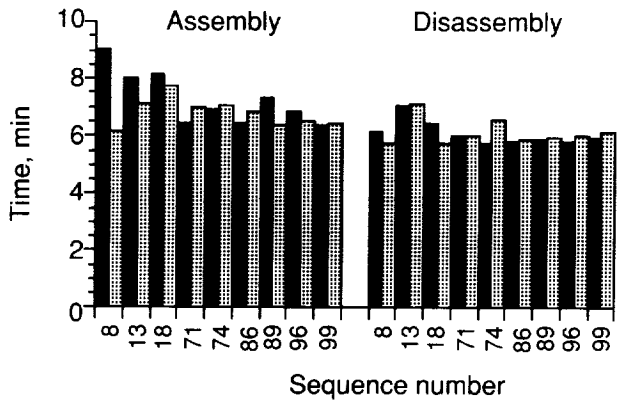

(d) 12_8 Path; capture installation.

Figure 19. Time required to assemble and disassemble struts via specific paths without force-torque controlled repositioning of the end effector and motion-base positioning.

Segment	Total time, min		Average time per strut, min	Portion of total time, percent
	Test A	Test B		
A	62.98	59.72	0.61	6.7
B	217.55	209.18	2.12	23.2
C	12.13	11.48	0.12	1.3
D	95.48	94.35	0.94	10.3
E	147.37	148.45	1.47	16.1
F	273.95	260.15	2.66	29.0
G	124.67	125.23	1.24	13.6
Total...	934.13 15hr 34min	908.56 15hr 8min	9.16	

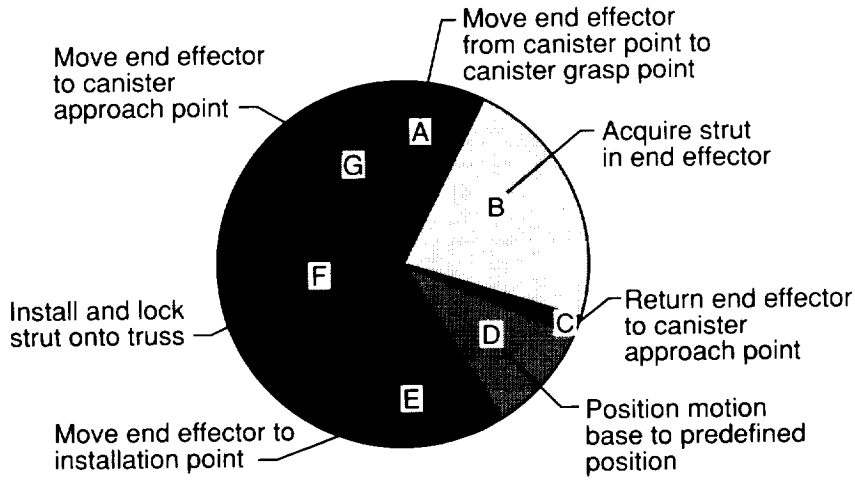

(a) Assembly.

Figure 20. Total time for successfully installed and removed struts.

Segment	Total time, min		Average time per strut, min	Portion of total time, percent
	Test A	Test B		
H	92.62	107.83	0.99	11.4
I	143.18	142.45	1.41	16.2
J	259.65	263.33	2.58	29.7
K	123.60	122.92	1.21	14.0
L	58.27	59.85	0.58	6.7
M	165.37	186.77	1.73	20.0
N	15.18	18.65	0.17	1.9
Total...	857.87 14hr 18min	901.80 15hr 2min	8.67	

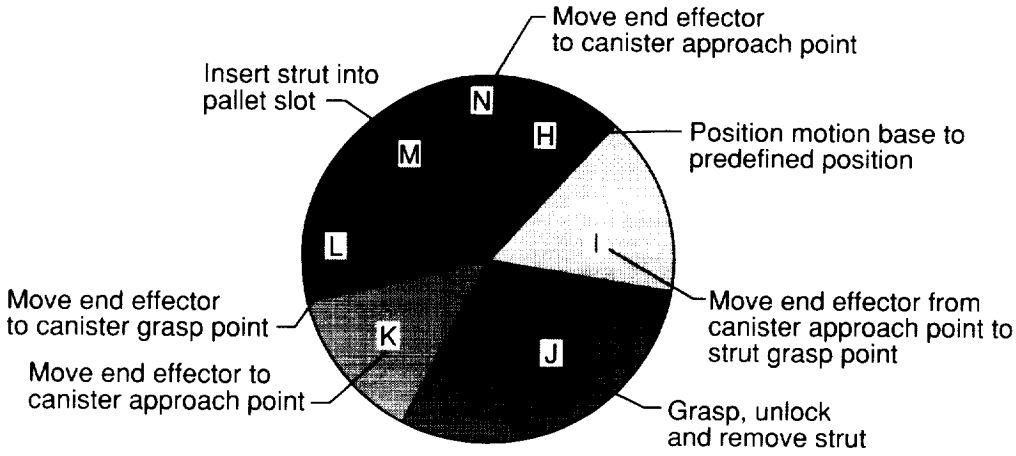

(b) Disassembly.

Figure 20. Concluded.

Segment	Total time, min	Average time per strut, min	Portion of total time, percent
A	61.2	0.6	13.64 - 11.10
B	51.0 - 102.0	0.5 - 1.0	11.36 - 18.50
C	10.2	0.1	2.27 - 1.90
D	0	0	0
E	153.0	1.5	34.09 - 27.80
F	51.0 - 102.0	0.5 - 1.0	11.36 - 18.50
G	122.4	1.2	27.27 - 22.20
Total...	448.8 - 550.8 7hr 28min - 9hr 10min	4.4 - 5.4	

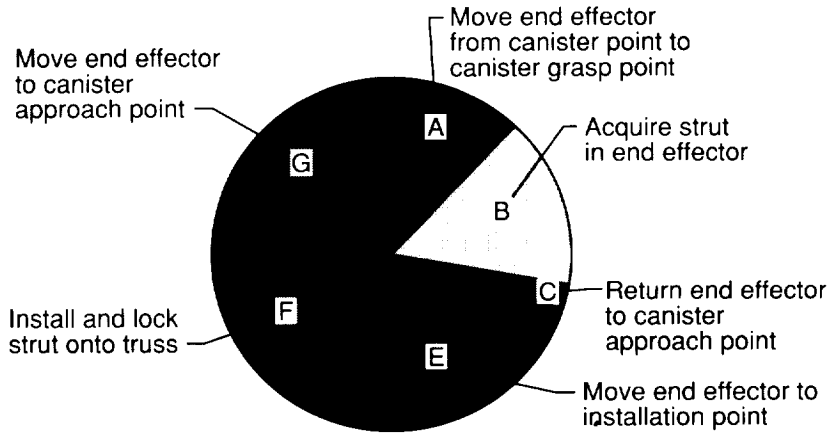

Figure 21. Estimated time to acquire and install strut in space.

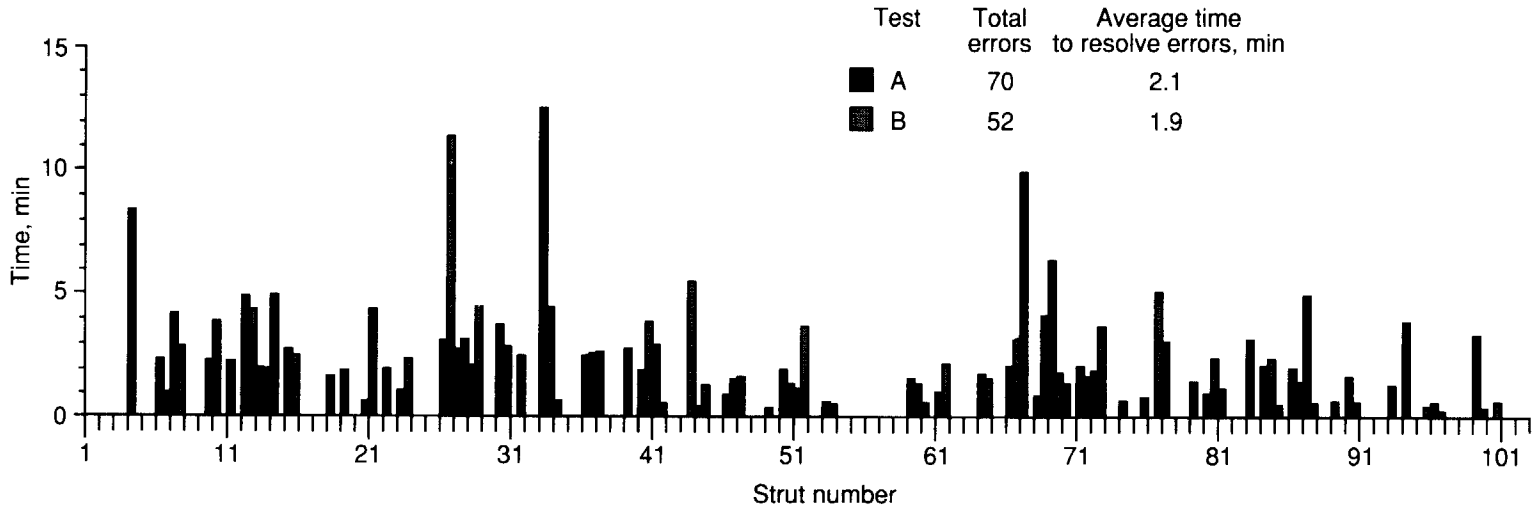

(a) Assembly tests.

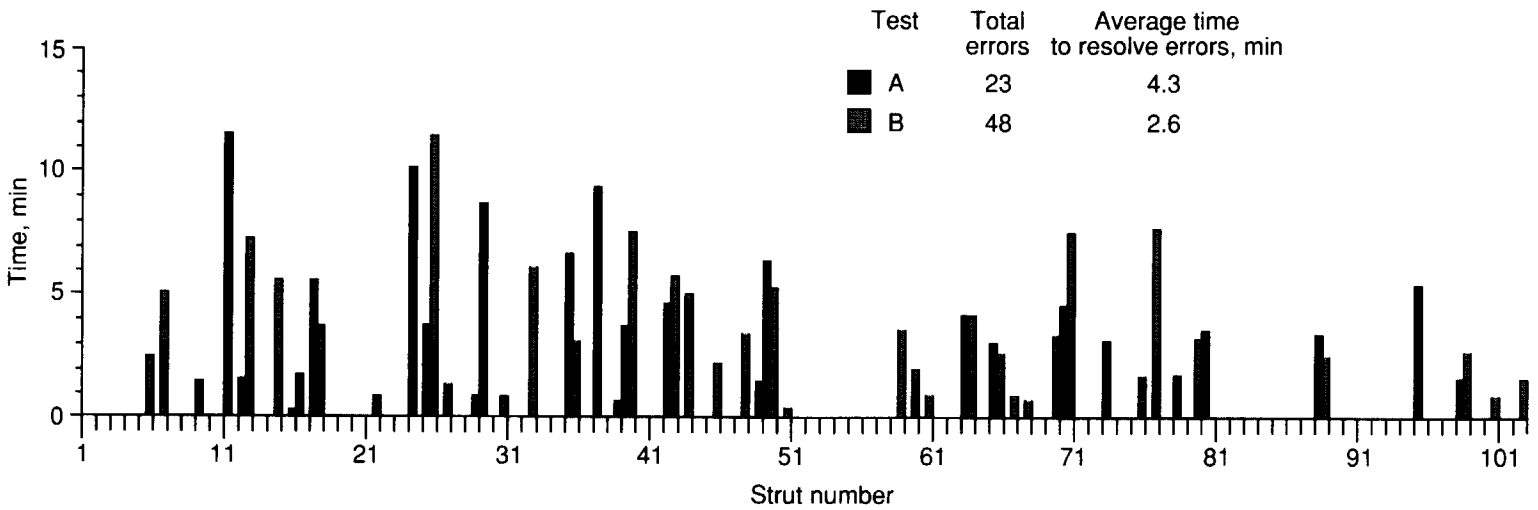

(b) Disassembly tests.

Figure 22. Time required by operator to identify and correct test errors.

REPORT DOCUMENTATION PAGE

Form Approved
OMB No. 0704-0188

1. AGENCY USE ONLY *(Leave blank)*	2. REPORT DATE	3. REPORT TYPE AND DATES COVERED
	July 1994	Technical Paper

4. TITLE AND SUBTITLE
Baseline Tests of an Autonomous Telerobotic System for Assembly of Space Truss Structures

5. FUNDING NUMBERS
WU 506-43-41-02

6. AUTHOR(S)
Marvin D. Rhodes, Ralph W. Will, and Coung Quach

7. PERFORMING ORGANIZATION NAME(S) AND ADDRESS(ES)
NASA Langley Research Center
Hampton, VA 23681-0001

8. PERFORMING ORGANIZATION REPORT NUMBER
L-17345

9. SPONSORING/MONITORING AGENCY NAME(S) AND ADDRESS(ES)
National Aeronautics and Space Administration
Washington, DC 20546-0001

10. SPONSORING/MONITORING AGENCY REPORT NUMBER
NASA TP-3448

11. SUPPLEMENTARY NOTES
Rhodes and Will: Langley Research Center, Hampton, VA; Quach: Lockheed Engineering & Sciences Company, Hampton, VA.

12a. DISTRIBUTION/AVAILABILITY STATEMENT
Unclassified Unlimited

Subject Category 18

12b. DISTRIBUTION CODE

13. ABSTRACT *(Maximum 200 words)*

Several proposed space missions include precision reflectors that are larger in diameter than any current or proposed launch vehicle. Most of these reflectors will require a truss structure to accurately position the reflector panels and these reflectors will likely require assembly in orbit. A research program has been conducted at the NASA Langley Research Center to develop the technology required for the robotic assembly of truss structures. The focus of this research has been on hardware concepts, computer software control systems, and operator interfaces necessary to perform supervised autonomous assembly. A special facility was developed and four assembly and disassembly tests of a 102-strut tetrahedral truss have been conducted. The test procedures were developed around traditional "pick-and-place" robotic techniques that rely on positioning repeatability for successful operation. The data from two of the four tests were evaluated and are presented in this report. All operations in the tests were controlled by predefined sequences stored in a command file, and the operator intervened only when the system paused because of the failure of an actuator command. The tests were successful in identifying potential pitfalls in a telerobotic system, many of which would not have been readily anticipated or incurred through simulation studies. Addressing the total integrated task, instead of bench testing the component parts, forced all aspects of the task to be evaluated. Although the test results indicate that additional developments should be pursued, no problems were encountered that would preclude automated assembly in space as a viable construction method.

14. SUBJECT TERMS	15. NUMBER OF PAGES
Truss structures; Robotic assembly; Space antennas; Automated assembly	45
	16. PRICE CODE: A03

17. SECURITY CLASSIFICATION OF REPORT	18. SECURITY CLASSIFICATION OF THIS PAGE	19. SECURITY CLASSIFICATION OF ABSTRACT	20. LIMITATION OF ABSTRACT
Unclassified	Unclassified		